

MICROCOPY RESOLUTION TEST CHART  
NATIONAL BUREAU OF STANDARDS-1963-A

ARO 18447.1-EG-H

(12)

VISCOELASTIC AND DAMPING PROPERTIES  
OF ARMOUR MATERIALS UNDER HYPERVELOCITY  
PENETRATION

FINAL REPORT  
for Research period May 15, 1981  
May 15, 1982

Dr. Czeslaw A. Broniarek  
December 31, 1982

U.S. Army Research Office  
Grant No. DAAG 29-81-G-0007.

DTIC  
JAN 20 1983  
H

SCHOOL OF ENGINEERING  
TUSKEGEE INSTITUTE, ALABAMA 36088

Approved for Public Release  
Distribution Unlimited

ADA 123562

DTIC FILE COPY

TABLE OF CONTENTS

1.	Statement of the Problem Studied . . . . .	1
2.	Experimental Procedure . . . . .	2
3.	Conclusions and recommendations . . . . .	3
4.	Acknowledgment . . . . .	4
5.	Appendix A Dissimilar Modeling . . . . .	
6.	Appendix B Experimental Determination of the Penetration Force.. . . .	
7.	Appendix C Design of Impact Force Transducer . . . . .	
8.	Appendix D The depth of penetration in a Target and maximum force in support plate for a lead-lead impact experiment . . . . .	
9.	References . . . . .	51

Accession For	
NTIS GRA&I	<input checked="" type="checkbox"/>
DTIC TAB	<input type="checkbox"/>
Unannounced Justification	
By _____	
Distribution/	
Availability Codes	
Dist	Avail and/or Special
A	

DTIC  
COPY  
INSPECTED  
2

REPORT DOCUMENTATION PAGE		READ INSTRUCTIONS BEFORE COMPLETING FORM
1. REPORT NUMBER 2nd Report	2. GOVT ACCESSION NO. AD-A123562	3. RECIPIENT'S CATALOG NUMBER
4. TITLE (and Subtitle) Viscoelastic and Damping Properties of Armour Materials under Hypervelocity Penetration.		5. TYPE OF REPORT & PERIOD COVERED Final Report, Dec. 31, 1982
7. AUTHOR(s) Dr. C. A. Broniarek		6. PERFORMING ORG. REPORT NUMBER
9. PERFORMING ORGANIZATION NAME AND ADDRESS Tuskegee Institute, School of Engineering Tuskegee Institute, AL 36088		8. CONTRACT OR GRANT NUMBER(s) Grant # :DAAG29-81-G-0007
11. CONTROLLING OFFICE NAME AND ADDRESS U. S. Army Research Office Post Office Box 12211 Research Triangle Park, NC 27709		10. PROGRAM ELEMENT, PROJECT, TASK AREA & WORK UNIT NUMBERS
14. MONITORING AGENCY NAME & ADDRESS (if different from Controlling Office)		12. REPORT DATE Dec. 31, 1982
		13. NUMBER OF PAGES
		15. SECURITY CLASS. (of this report) Unclassified
		15a. DECLASSIFICATION/DOWNGRADING SCHEDULE
16. DISTRIBUTION STATEMENT (of this Report)  Approved for public release; distribution unlimited.		
17. DISTRIBUTION STATEMENT (of the abstract entered in Block 20, if different from Report)  NA		
18. SUPPLEMENTARY NOTES The view, opinions, and/or findings contained in this report are those of the author(s) and should not be construed as an official Department of the Army position, policy, or decision, unless so designated by other documentation.		
19. KEY WORDS (Continue on reverse side if necessary and identify by block number) Hypervelocity, Penetration, Piercing, Viscoelastic, Impact, Strain Rate, Shock, Heat of Fusion, Crater, Vaporization, Wave propagation, Phase transformation, Disimilar Scaling, <i>Adaptive</i>		
20. ABSTRACT (Continue on reverse side if necessary and identify by block number) In this report, the theoretical and experimental verification of dissimilar modeling and scaling laws for a hypervelocity impact and penetration mechanism are presented. The impact test apparatus was designed, built and used for generation of the data for the verification of the scaling laws by means of dissimilar materials of the model and prototype. Two types of impact force transducers were developed, employed either membrane or segment of the tube as a sensing element. The second type occurred to be very effective for these applications. The results of computation and experimentation are presented. The developed method of an indirect		

20. ABSTRACT (Cont'd)

↘ measuring of the instantaneous penetration and penetration force was successfully used in this research. ↗

## 1. STATEMENT OF THE PROBLEM STUDIES

The attempt of an adequate characterization of an armour plate material impacted by a striker (projectile) at a high velocity exceeding the sound velocity in the armour plate (target). Emphasis is placed on scaling and similarity condition between laboratory scaled model and prototype system (actual striker-armour system). It has been shown that the laboratory test results on the dissimilar materials can be used for the characterization of the material of the armour and striker under high strain rate (about  $10^6 \text{ sec}^{-1}$ ). Specifically, the tests were performed on lead, copper and aluminum and the results were transformed in the actual steel armour material. The modeling and scaling procedure is presented in Appendix A. The laboratory test apparatus is described in Appendix B. The impact force transducers being used in this research are presented in Appendix C. The calculations of the depth of penetration and maximum force are presented in Appendix D.

More work needs to be done in this research. The all results are obtained during the first year of an intensive work in this project. Some of the measuring transducers and equipment arrived after the contract was terminated in May 1982. Therefore we could not accomplish what was planned for this part of the research.

The experimental test apparatus was designed and fabricated, including force transducers, photocells, remote triggering device, electronic circuits, etc. The dual channel digital signal analyzer (HP 5225) was used for data storage and recording.

## 2. EXPERIMENTAL TEST PROCEDURE

The essential part of the testing apparatus is a modified Remington 30-06 caliber rifle with a smooth barrel. The supporting frame baffle plates, remotely controlled triggering device, target specimen holder, etc. are shown in Figure 1. A low power laser was used for an accurate aiming during testing. See Figs. 5 and 6. The electronic equipment such as FFT digital system, 4 channel storage oscilloscopes, polaroid cameras, etc. are shown in Figure 7.

A typical frequency spectrum record is shown in Figure 8 and force response is shown in Figure 9.

The creaters obtained on lead, aluminum and brass are shown in Figures 10, 11. A few examples of experimental data are shown in Figures 12 - 15.



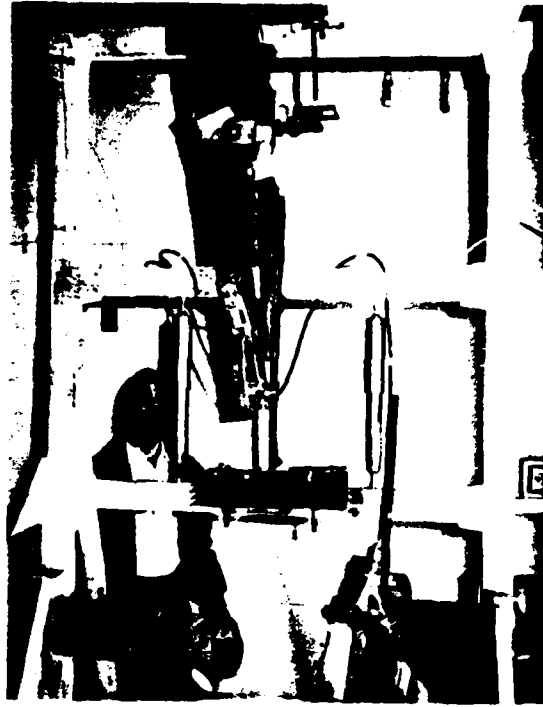


Fig. 1. The close view on the rifle holder, prism, baffle plates, and the upper frame.

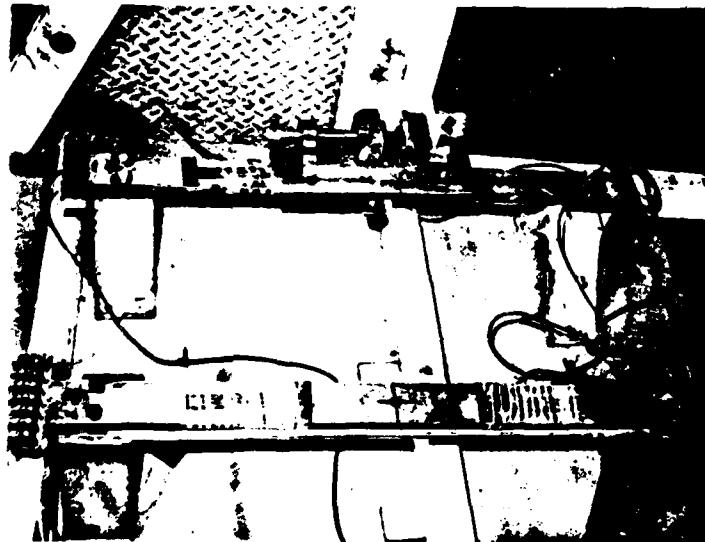


Fig. 2. The force transducers supporting the target specimens.

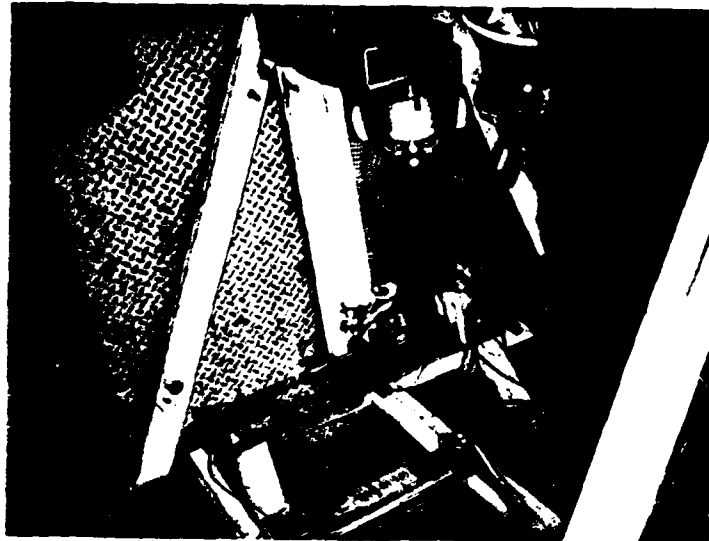


Fig. 3. The target specimen holders fixed to the force transducers.



Fig. 4. The shock absorber and triggering force cell.

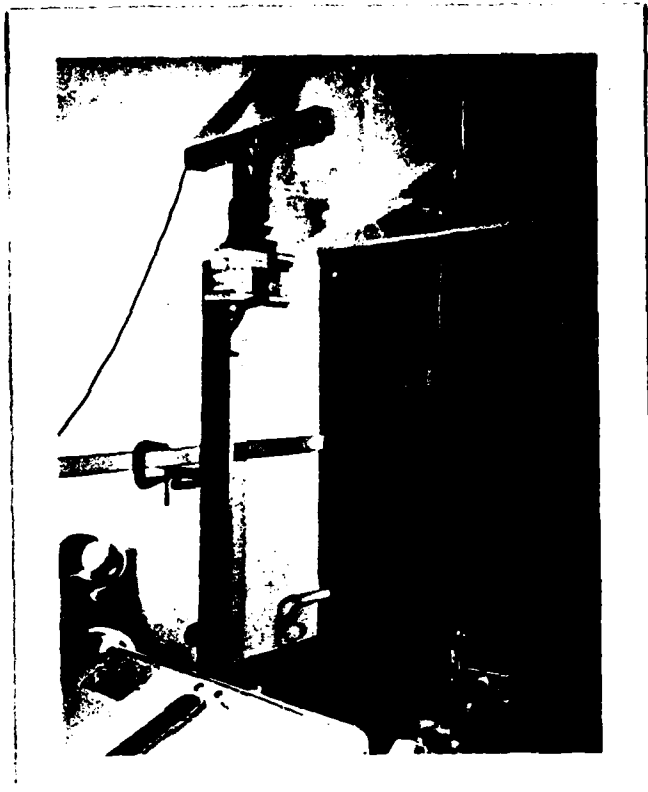


Fig. 5. Laser aiming device.

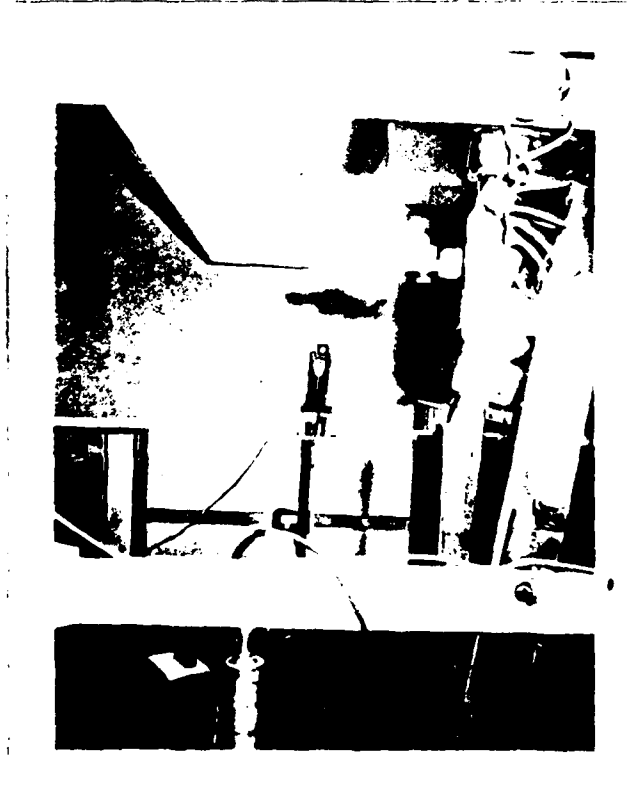


Fig. 6. The laser incorporating with the prism.

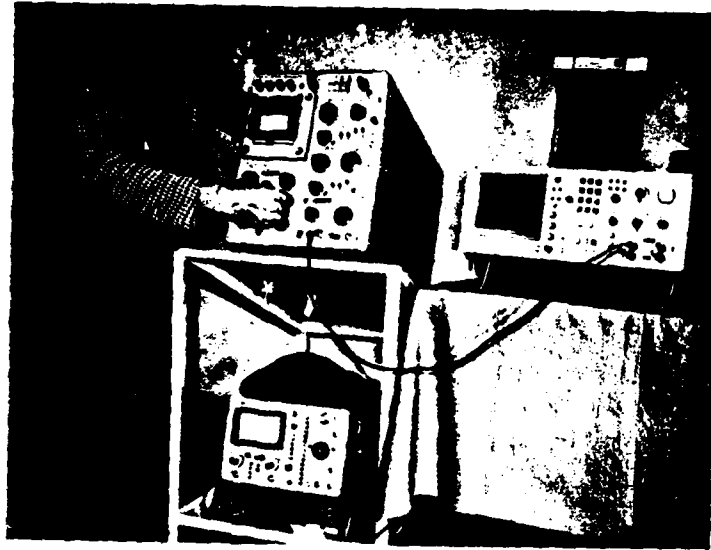


Fig. 7. Storage oscilloscope and Hewlett-Packard frequency analyzer.

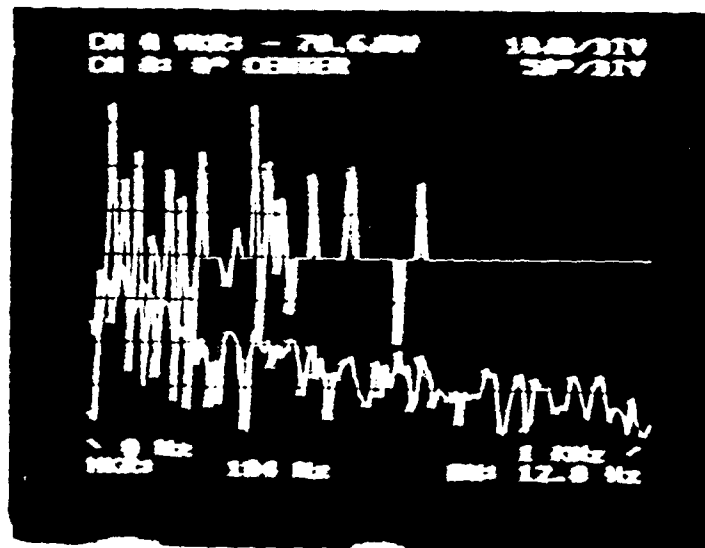


Fig. 8. Typical frequency spectrum sample.

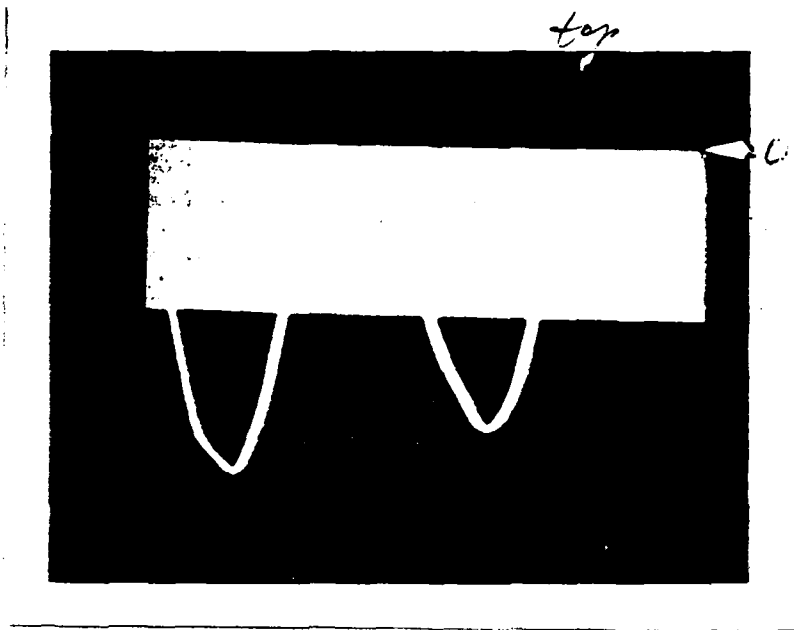


Fig. 9. Typical force response of the penetration of the lead specimen

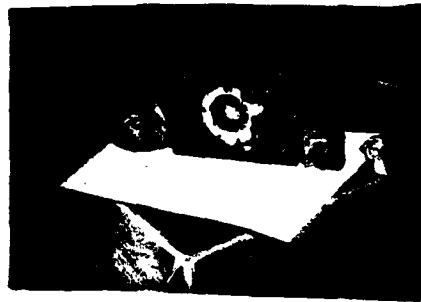


Fig. 10. Three typical craters on brass, lead, and aluminum at 2.1 cm/sec.

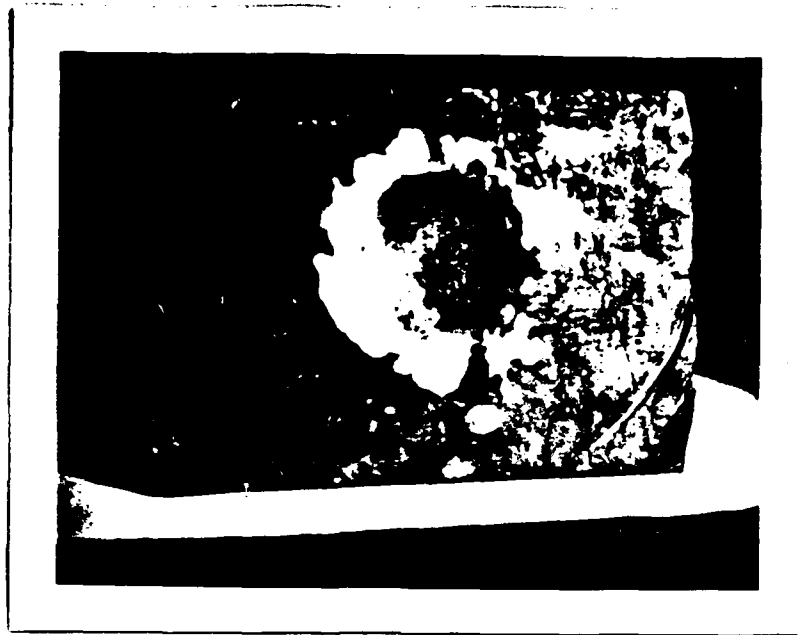


Fig. 11. Crater in the lead target

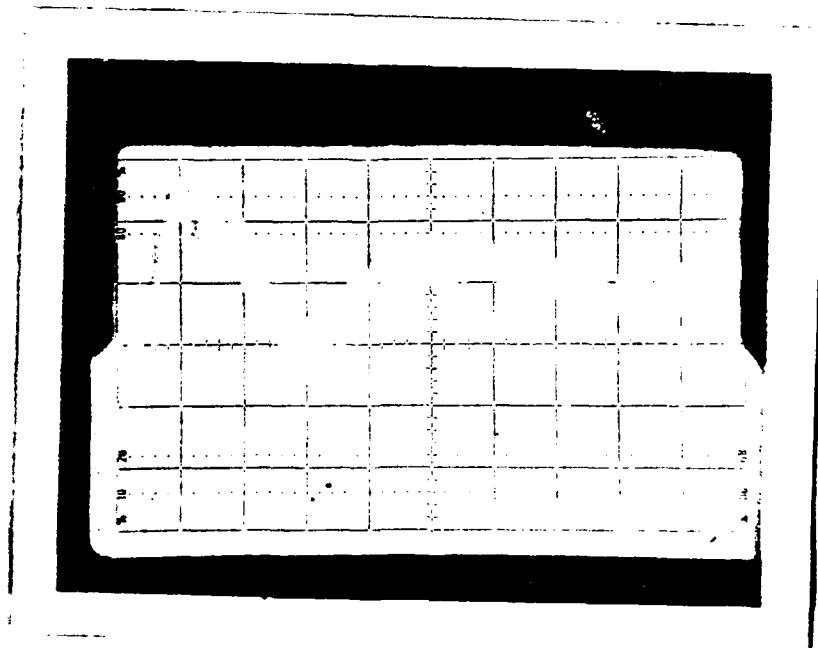


Fig. 12. Force response from the test on the lead specimen penetrated by the lead penetrator at 2.1 km/sec. 1.5 volts/div., 10ns/div.

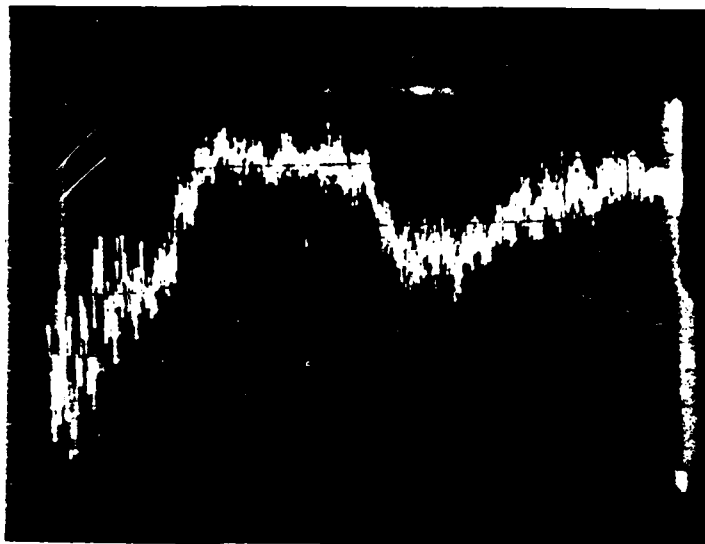


Fig. 13. Same as in Fig. 12 except the copper jacket lead penetrator was used. 5 volts/div., 5 ms/div.

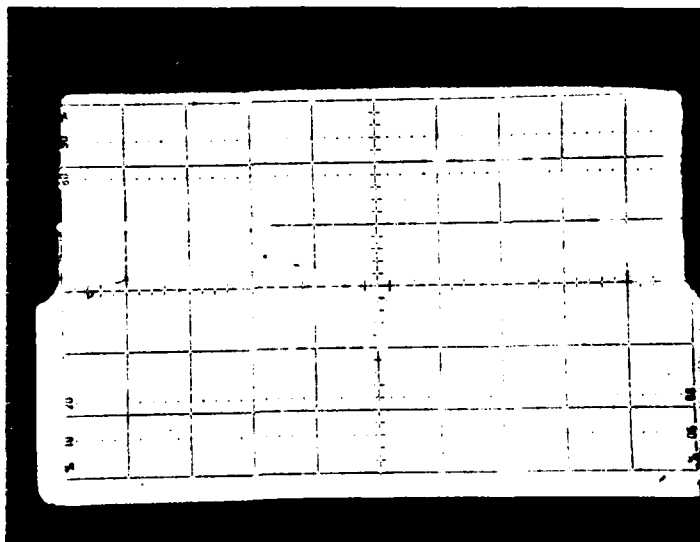


Fig. 14. Force response from the test on aluminum specimen. Lead penetrator. 5 volts/div. 5 ms/div.

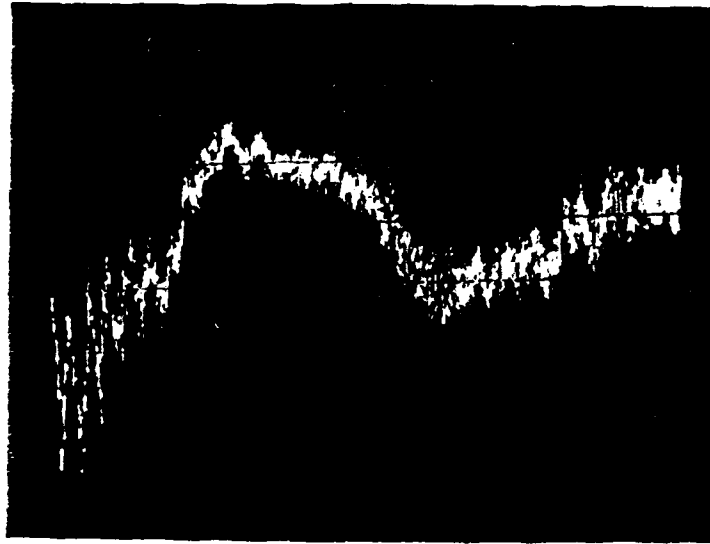


Fig. 15. Same as in Fig. 14, but copper jacket - lead penetrator was used. 5 volts/div., 5 ms/div.



### 3. Conclusions and recommendations:

The following conclusions and recommendations are based on the information and analysis given in this report.

1. The armour material behavior under high velocity impact by a striker can be determined by means of laboratory experiment performed on the scaled model with different than prototype materials such as lead and copper.

2. The armour support stiffness is negligible if the period of natural frequency of the mass of the armour on the supporting spring is at least 20 times longer than an impact time.

3. More analytical and experimental work needs to be done on materials and configurations to validate the scaling law.

#### ACKNOWLEDGEMENT

The author wishes to express his sincere thanks to the U.S. Army Research Office and personally to Dr. Edward A. Saibel, for the aid received to support this research through grant No. DAAG 29 81-G-0007.

The author expresses his appreciation to the Department of Mechanical Engineering and Grant Management Office at Tuskegee Institute, for their support.

The work done by Mr. Raymond Bus-Kwofie, a graduate student, is acknowledged.

APPENDIX A  
DISSIMILAR MODELING AND SCALING OF HYPERVELOCITY PENETRATION  
AND PIERCING

A1. INTRODUCTION

In this report the impact is defined as a collision of two bodies: The striker or impactor and the armour plate or target. In the low impact velocity regime ( 250 m/s) the local indentations or penetrations are strongly coupled to the overall deformation of the entire armour plate (Ref. 1). As the striking velocity increases to the order of magnitude of about 1,500 m/sec. the response of the armour is dominated by the dynamic behavior of the armour material within a small zone (approximately 2 - 3 striker diameters) of the impact area. Loading and reaction times are on the order of milliseconds. the increasing impact velocity to 2,000 - 3,000 m/sec. result in localized pressures which exceed significantly the interatomic bounding forces resulting in instantaneous liquification of the materials in the early stages of impact. At ultra-high velocities exceeding 12,000 m/sec. energy deposition occurs at such a high rate that an explosive vaporization of striker and armour materials results.

The test results obtained by firing 1/8 in tungsten-carbide spheres into lead targets at various speeds are shown in Figure 1. The ordinate of the figure is a dimensionless depth of penetration  $P/d$ , and the abscissa is a dimensionless velocity of impact. Photographic examples of a failure mode in one of the three categories after sectioning are inserted over the portion of the graph in Figure 1 to which they belong (Reference 2).

The characterization of the impact with respect to striking velocity  $V$  and strain rate ( $\dot{\epsilon} = \frac{d\epsilon}{dt}$ ) is shown in Table 1 (Reference 1). This characterization is very flexible since the deformation processes under impact depend on many other parameters in addition to impact velocity such as: Geometry of a striker and armour plate, elastic-plastic shock wave propagation, hydrodynamic flow, work hardening, thermal and frictional effects, and the initiation and preparation of failure in striker and armour materials.

By definition, penetration is an entrance of a projectile (striker) into a target without completing its passage through the armour (Ref. 1). Perforation implies the complete piercing of a target by the projectile and occurs in several to several hundred milliseconds.

Impacted armour plate may fail in a variety of ways. Figure 2 taken from Reference 1, shows some of the modes for thin and intermediate thickness targets.

In the hypervelocity regime of impact, the most important physical parameter are specific heat, latent heat of fusion, melting point and density. (Ref. 2). The corresponding nondimensional parameters obtained from Buckingham's  $\Pi$  theorem are

$$\pi_6 = \frac{\rho_P}{\rho_T}, \quad \pi_{11} = \frac{\theta_P}{\theta_T}, \quad \pi_{12} = \frac{n_P}{n_T}, \quad \pi_{13} = \frac{C_P}{C_T}, \quad \pi_{14} = \frac{V^2}{n_T}$$

$$\pi_{15} = \frac{\theta_t C_t}{n_t}$$

It can be argued that  $\pi_{11}$ ,  $\pi_{12}$ , and  $\pi_{13}$  are not significant because the amount of penetrator material heated and melted is small compared with the amount of target material melted.

The most significant  $\pi$  terms therefore are  $\pi_6$ ,  $\pi_{14}$  and  $\pi_{15}$ . For most metals there is a correlation between the speed of sound and the latent heat of fusion  $n$ . See Fig. 3.

The correlation is given by  $a^2 = 95n$ .

The group  $\pi_{14}$  can therefore be replaced by  $\frac{V}{a_T}$

The work of Summers and Charters, (Ref. 2), shows that  $\pi_6$  and  $\pi_{14}$  can be lumped into

$$\frac{\rho_P}{\rho_T} \frac{V}{a_T}$$

When the nondimensional penetration  $P/d$  is plotted against the correlation is

$$\frac{\rho_P V}{\rho_T a_T}$$

$$\frac{P}{d} = 2.28 \left( \frac{\rho_P}{\rho_T} \frac{V}{a_T} \right)^{\frac{2}{3}}$$

(A1)

Here  $a_t$  is the bar velocity of sound. it is more practical to take  $a_t$  as the bulk velocity. When Summers and charter's graph is replotted the correlation will be

$$\frac{P}{d} = 2.755 \left( \frac{\rho_P V}{\rho_T a_t} \right)^{0.6273}$$

(A2)

Using the above result, tables of non-dimensional depth of penetration versus velocity for various targets and penetrators can be determined.

Another example is with an aluminum penetrator. Aluminum is so light that it requires more than 4 times the speed to do the same damage as a lead penetrator on a steel target.

It would be interesting to find the ratio of energy that goes

into heating and melting the target. The rest of the energy presumably goes to impact kinetic energy to the molten material, cause vibration, induce a shock wave in the material and cause strain energy insufficient to melt the material.

The material presented here gives us a rough indication of the velocities we should expect for various penetrations and relies heavily on the work of Summers and Charters as presented in Ref. 2. More work has to be done to determine whether their results truly apply to various material combinations and whether in these cases we can ignore the  $\Pi$  terms they ignored.

The group  $\Pi_{15}$  is very important in that it gives a measure of the amount of heat used in raising temperature by that used in melting the material. It is a dimensionless term that has to be satisfied for proper scaling. For all the metals scaling is more or less satisfied for this term but not so for wax. The sensitivity of dimensionless penetration to  $\Pi_{15}$  has to be determined to make wax applicable as a model for other metals.

A2. Calculation of fictitious speed of sound for wax for use in Summers and Charter Graph

The heat of fusion for a wax is

$$n_{\text{wax}} = 1.3 \times 10^5 \text{ J/kg.}$$

Functional relationships are as follows:

$$a^2 = 95 L.$$

$$a^2 = 95 \times 1.3 \times 10^5 = 12.35 \times 10^6 \text{ m}^2/\text{S}^2$$

$$a_{\text{eq}} = \underline{3.514 \times 10^3 \text{ m/S}}$$

The only factor left to be scaled is thus

$$\frac{\theta_t C_t}{n_t} = \Pi_{15}$$

For metals they are roughly the same 2.3

For wax  $\frac{61.8}{42.3} \times C_t$  or

$$\left( \frac{\theta_t C_t}{n_{t \text{ wax}}} \right) = 1.46099 C_t$$

A =

A3. Calculations of the parameters for various combinations between impactor and armour materials and dimensions.

Material for Model Selected:

<u>Target</u>	<u>Projectile</u>
Lead	High carbon steel.
Copper	High carbon steel.

Material for Prototype Selected:

<u>Target</u>	<u>Projectile</u>
High carbon steel	High carbon steel

DATA

Density of Lead	=	711.70 lb/cu.ft.
Density of Copper	=	557.50 lb/cu.ft.
Density of High Carbon Steel	=	489.45 lb/cu.ft.
Velocity of sound in lead	=	7086.96 ft/sec.
Velocity of sound in copper	=	15.617.56 ft/sec.
Velocity of sound in High Carbon Steel	=	19.489.14 ft/sec.

From Figure 4 we have the relation for a model (subscript Mo)

$$\left(\frac{P}{d}\right) = 2.28 \left(\frac{\rho_p}{\rho_t}\right)_{M_0}^{\frac{2}{3}} \left(\frac{V}{a_t}\right)_{M_0}^{\frac{2}{3}} \quad (A3)$$

$\frac{P}{d}$  = Depth of penetration.

$\frac{\rho_p}{\rho_t}$  = Ratio of densities of projectile and target

$\frac{V}{a_t}$  = Ratio of impact velocity to velocity of sound on target material

Let 
$$\left(\frac{\rho_p}{\rho_t}\right)_{Pr} = \lambda \left(\frac{\rho_p}{\rho_t}\right)_{M_0} \quad (A4)$$

is the scaling factor equal to

$$\lambda = \left(\frac{\rho_p}{\rho_t}\right)_{Pr} / \left(\frac{\rho_p}{\rho_t}\right)_{M_0} \quad (A5)$$

Multiplying and dividing right hand side of equation A3, we have,

$$\left(\frac{P}{d}\right)_{M_0} = 2.28 \left(\frac{\rho_p}{\rho_t}\right)_{M_0}^{\frac{2}{3}} \left(\frac{V}{a_t}\right)_{M_0}^{\frac{2}{3}} \lambda^{\frac{2}{3}} \frac{1}{\lambda^{\frac{2}{3}}} \quad (A6)$$

We can determine the impact velocity of the projectile in the prototype. Assuming the same depth of penetration, i.e.

$$\left(\frac{P}{d}\right)_{M_0} = \left(\frac{P}{d}\right)_{Pr} \quad (A7)$$

From Eq. (A4) we have

$$\left(\frac{\rho_p}{\rho_t}\right)_{M_0}^{\frac{2}{3}} \lambda^{\frac{2}{3}} = \left(\frac{C_p}{C_t}\right)_{Pr}^{\frac{2}{3}} \quad (A8)$$

and

$$\left(\frac{P}{d}\right)_{Pr} = 2.28 \left(\frac{\rho_p}{\rho_t}\right)_{Pr}^{\frac{2}{3}} \frac{1}{\lambda^{\frac{2}{3}}} \left(\frac{V}{a_t}\right)_{M_0}^{\frac{2}{3}} \quad (A9)$$

From Eq. (A3) we get

$$\left(\frac{P}{d}\right)_{Pr} = 2.28 \left(\frac{\rho_p}{\rho_t}\right)_{Pr}^{\frac{2}{3}} \left(\frac{V}{a_t}\right)_{Pr}^{\frac{2}{3}} \quad (A10)$$

comparing Eq. (A10) with Eq. (A9) we obtain.

$$\left(\frac{V}{a_t}\right)_{M_0}^{\frac{2}{3}} \frac{1}{\lambda^{\frac{2}{3}}} = \left(\frac{V}{a_t}\right)_{Pr}^{\frac{2}{3}} \quad (A11)$$

$$\left(\frac{V}{a_t}\right)_{Pr} = \frac{1}{\lambda} \left(\frac{V}{a_t}\right)_{M_0} \quad (A12)$$

and

$$\left(\frac{V}{a_t}\right)_{Pr} = \frac{(V/a_t)_{M_0}}{(\rho_p/\rho_t)_{Pr} / (c_p/\rho_t)_{M_0}} \quad (A13)$$

(A14)

Assuming depth of penetration in model we can find the velocity of impact for the penetrator or projectile. We can also find the impact velocity of projectile in the case of prototype for the same depth of penetration.

For  $(P/d) = 0.2$   
Model: Target - Lead  
Projectile - High Carbon Steel.

$$\left(\frac{P}{d}\right)_{M_0} = 2.87 \left(\frac{\rho_P}{\rho_T}\right)_{M_0}^{\frac{2}{3}} \left(\frac{V}{a_t}\right)^{\frac{2}{3}}$$

$$0.2 = 2.87 \left(\frac{489.45}{7.11.70}\right)^{\frac{2}{3}} \left(\frac{V}{a_t}\right)^{\frac{2}{3}}$$

$$\left(\frac{V}{a_t}\right) = 0.0894$$

∴ Velocity of the projectile = 189.57 ft/sec.

Prototype:

Target Material : High carbon steel  
Projectile material : High carbon steel

$$\left(\frac{V}{a_t}\right)_{P_T} = \left(\frac{V}{a_t}\right)_{M_0} \cdot \frac{(\rho_P/\rho_T)_{M_0}}{(\rho_P/\rho_T)_{P_T}}$$

$$= 0.026 \times 0.687 = 0.0179$$

$$V_p = 0.0179 \cdot (a_t)_{P_T} = 348.48 \text{ ft/sec}$$

2. For  $(P/d) = 0.4$  (Model)

$$\left(\frac{P}{d}\right)_{M_0} = 2.87 \left(\frac{\rho_P}{\rho_T}\right)^{\frac{2}{3}} \left(\frac{V}{a_t}\right)^{\frac{2}{3}}$$



$$0.4 = 2.87 (.688)^{\frac{2}{3}} \left( \frac{V}{a_t} \right)^{\frac{2}{3}}$$

$$\left( \frac{V}{a_t} \right)^{\frac{2}{3}} = \frac{0.4}{2.87} \frac{1}{0.7793} = .1788$$

$$\frac{V}{a_t} = 0.0756$$

$$\therefore V = 0.0756 \times (a_t)_{M_0} = 535.81 \text{ ft/sec.}$$

Velocity of impact of projectile = 535.81 ft/sec.

Prototype

$$\left( \frac{V}{a_t} \right)_{Pr} = \left( \frac{V}{a_t} \right)_{M_0} \left( \frac{(\rho_p/\rho_t)_{M_0}}{(\rho_p/\rho_t)_{Pr}} \right), \quad \left( \frac{\rho_p}{\rho_t} \right)_{M_0} = .6877$$

$$\left( \frac{V}{a_t} \right)_{Pr} = 0.6877 \times \left( \frac{V}{a_t} \right)_{M_0} \quad \left( \frac{\rho_p}{\rho_t} \right)_{Pr} = 1$$

$$= 0.6877 \times 0.0756 = 0.05199$$

$$V_{Pr} = 1013.27 \text{ ft/sec.}$$

Velocity of impact in case of prototype = 1013.27 ft/sec.

For  $(P/d) = 0.6$

$$.6 = 2.236 \left( \frac{V}{a_t} \right)_{M_0}^{\frac{2}{3}}$$

$$\text{hence } V = 985.09 \text{ ft/sec.}$$

Prototype:  $\left(\frac{V}{a_t}\right)_{Pr} = \left(\frac{V}{a_t}\right)_{M_0} \times 0.6877$ ;  $\left(\left(\frac{P}{\rho_t}\right) = 0.6877\right)$   
 $= 0.139 \times 0.6877$   
 $\therefore V_{Pr} = 1862.97 \text{ ft/sec.}$

Velocity of Projectile in prototype = 1862.97 ft/sec.

For  $\frac{P}{d} = 0.8$

$$\left(\frac{V}{a_t}\right)_{M_0} = 0.2140$$

$$\therefore V_{M_0} = 1516.65 \text{ ft/sec.}$$

Velocity of Projectile on model = 1516.65 ft/sec.

Prototype

$$\left(\frac{V}{a_t}\right)_{Pr} = \left(\frac{V}{a_t}\right)_{M_0} \times 0.6877$$

$$= 0.2140 \times 0.6877 = 0.1471$$

$$V_{Pr} = 2868.17 \text{ ft/sec.}$$

Velocity of Projectile in Prototype = 2868.17 ft/sec.

For  $\frac{P}{d} = 1 = 2.236 \left(\frac{V}{a_t}\right)_{M_0}^{\frac{2}{3}}$

$$\left(\frac{V}{a_t}\right) = 0.299$$

$$\therefore V = 219.3 \text{ ft/sec.}$$

Velocity of the target in model = 2119.3 ft/sec.

Prototype

$$\left(\frac{V}{a_t}\right)_{Pr} = \left(\frac{V}{a_t}\right)_{M_0} \times 0.6877$$

$$= 0.299 \times 0.6877$$

$$V_p = 4007.40 \text{ ft/sec.}$$

Velocity of Projectile in Prototype = 4007.40 ft/sec.

For

$$P/d = 1.2$$

$$1.2 = 2.236 \left( \frac{V}{a_t} \right)_{M_0}^{\frac{2}{3}}$$

$$\left( \frac{V}{a_t} \right)^{\frac{2}{3}} = \frac{1.2}{2.236}, \quad \left( \frac{V}{a_t} \right)_{M_0} = 0.3931$$

$$\therefore V = 2786.27 \text{ ft/sec.}$$

Velocity of Projectile of Model = 2786.27 ft/sec.

Prototype:

$$\left( \frac{V}{a_t} \right)_{pr} = \left( \frac{V}{a_t} \right)_{M_0} \times 0.6877$$

$$= 0.3931 \times 0.6877 = 0.2703$$

$$V = 5268.59 \text{ ft/sec.}$$

Velocity of Projectile in the case of Prototype = 5268.59 ft/sec.

For  $P/d = 1.4$

$$1.4 = 2.236 \left( \frac{V}{a_t} \right)^{\frac{2}{3}}$$

$$\left( \frac{V}{a_t} \right) = 0.4954$$

$$\therefore V = 3511.1 \text{ ft/sec.}$$

Velocity of projectile in the case of model = 3511.1 ft/sec.

Prototype:

$$\left(\frac{V}{a_t}\right)_{pr} = \left(\frac{V}{a_t}\right)_{M_0} \times 0.6877 = 0.4954 \times 0.6877$$
$$= 0.3406$$
$$\therefore V = 6639.68 \text{ ft/sec.}$$

Velocity of the Projectile in the case of Prototype

$$= 0.3406$$

Velocity of the Projectile in the case of Prototype

$$= 6639.68 \text{ ft/sec.}$$

For Model:

Target

Copper - material

Projectile

High Carbon Steel

For Prototype:

Target material

High carbon steel

Projectile material

High carbon steel.

For  $(P/d)$  of 0.2

Model:

$$\left(\frac{P}{d}\right)_{M_0} = 2.87 \left(\frac{\rho_p}{\rho_t}\right)_{M_0}^{\frac{2}{3}} \left(\frac{V}{a_t}\right)_{M_0}^{\frac{2}{3}}$$

$$0.2 = 2.87 \times 0.917 \left(\frac{V}{a_t}\right)_{M_0}^{\frac{2}{3}}$$

$$0.2 = 2.631 \left(\frac{V}{a_t}\right)_{M_0}^{\frac{2}{3}}$$

$$\left(\frac{V}{a_t}\right)_{M_0} = 0.0209, \quad V_{M_0} = 327.32 \text{ ft/sec.}$$

Velocity of Projectile in the case of model = 327.32 ft/sec.

Prototype

$$\left(\frac{V}{a_t}\right)_{pr} = \left(\frac{V}{a_t}\right)_{M_0} \frac{(\rho_p/\rho_t)_{M_0}}{(\rho_p/\rho_t)_{pr}} = \left(\frac{V}{a_t}\right)_{M_0} \left(\frac{\rho_p}{\rho_t}\right)_{M_0}$$
$$= 0.878 \left(\frac{V}{a_t}\right)_{M_0}$$

$$\left(\frac{V}{a_t}\right)_{pr} = 0.878 \times 0.209 = .1835$$

$$\therefore V_{pr} = 3576.37 \text{ ft/sec.}$$

Velocity of the Projectile in the case of Prototype = 3576.37 ft/sec.

For

$$P/d = .4$$

$$.4 = 2.631 \left(\frac{V}{a_t}\right)_{M_0}^2$$

$$\therefore V_{M_0} = 921.44 \text{ ft/sec}$$

Velocity of Projectile in the case of model = 921.44 ft/sec.

Prototype:

$$\left(\frac{V}{a_t}\right)_{pr} = 0.878 \left(\frac{V}{a_t}\right)_{M_0}$$

$$V_{pr} = 1009.58 \text{ ft/sec.}$$

Velocity of Projectile in th case of Prototype = 1009.58 ft/sec.

For

$$P/d = .6$$

$$\left(\frac{V}{a_t}\right)_{M_0} = .109 \quad \therefore V = 1702.31$$

Velocity of Projectile in Model = 1702.31 ft/sec.

For Prototype:

$$\left(\frac{V}{a_t}\right)_{pr} = 0.878 \left(\frac{V}{a_t}\right)_{Mo}$$

$$V_{pr} = 1865.19$$

Velocity of Projectile in the case of Prototype = 1865.19 ft/sec.

For

$$P/d = 0.8$$

$$0.8 = 2.631 \left(\frac{V}{a_t}\right)_{Mo}^{\frac{2}{3}}$$

$$\left(\frac{V}{a_t}\right) = 0.168 \quad \therefore V = 2618.59 \text{ ft/sec}$$

Velocity of Projectile in the case of Model = 2618.59 ft/sec.

Prototype:

$$\left(\frac{V}{a_t}\right)_{pr} = 0.878 \left(\frac{V}{a_t}\right)_{Mo}$$

$$= 0.148$$

$$\therefore V = 2874.73 \text{ ft/sec.}$$

Velocity of Projectile in the case of Prototype = 2874.73 ft/sec.

For

$$P/d = 1.0$$

$$1.0 = 2.631 \left(\frac{V}{a_t}\right)_{Mo}^{\frac{2}{3}}$$

$$\therefore V = 3659.56 \text{ ft/sec.}$$

Velocity of Projectile in the case of Model = 3659.56 ft/sec.

Prototype:

$$\left(\frac{V}{a_t}\right)_{pr} = 0.878 \left(\frac{V}{a_t}\right)_{Mo}$$

A(12)

$$\left(\frac{V}{a_t}\right)_{pr} = .205$$

$$\therefore V = 4004.03 \text{ ft/sec.}$$

Velocity of Projectile in the case of Prototype = 4004.03 ft/sec.

For

$$P/d = 1.2$$

$$1.2 = 2.631 \left(\frac{V}{a_t}\right)_{M_0}^{2/3}$$

$$\therefore = 4810.52 \text{ ft/sec.}$$

Velocity of projectile in the case of Model = 4810.52 ft/sec.

Prototype:

$$\left(\frac{V}{a_t}\right)_{pr} = .878 \left(\frac{V}{a_t}\right)_{M_0}$$

$$= .2704$$

$$V_p = 5270.33 \text{ ft/sec.}$$

Velocity of Projectile in the case of Prototype = 5270.33 ft/sec.

For.  $P/d = 1.4$

$$1.4 = 2.631 \left(\frac{V}{a_t}\right)_{M_0}^{2/3}$$

$$\left(\frac{V}{a_t}\right)_{M_0} = .388$$

$$\therefore V = 6062.11 \text{ ft/sec.}$$

Velocity of Projectile in the case of Model = 6062.11 ft/sec.

Prototype:

$$\left(\frac{V}{a_t}\right)_{pr} = .878 \times \left(\frac{V}{a_t}\right)_{M_0}$$

$$V_{pr} = 6682.99 \text{ ft/sec.}$$

↓ (1.2)

Velocity of Projectile in the case of Prototype = 6682.99 ft/sec.

We have the relation

$$\left(\frac{v}{a_t}\right)_{pr} = \left(\frac{v}{a_t}\right)_{Mo} \left(\frac{(\rho_p/\rho_t)_{Mo}}{(\rho_p/\rho_t)_{pr}}\right)$$

$$\text{Let } \lambda = \frac{(\rho_p/\rho_t)_{Mo}}{(\rho_p/\rho_t)_{pr}}$$

For various values of  $\lambda$ , assuming the velocity of the Projectile in Model we can find the corresponding values of impact velocity in the case of prototype. i.e. for a given value of  $(v/a_t)_{Mo}$  We can find the value of  $(v/a_t)_{pr}$  for a given value of  $\lambda$ .

For  $\lambda = 0.2$

1.	0.2	=	$(v/a_t)_{Mo}$	0.04	=	$(v/a_t)_{pr}$
2.	0.4			0.08		
3.	0.6			0.12		
4.	0.8			0.16		
5.	1.0			0.2		
6.	1.2			0.24		
7.	1.4			0.28		
8.	1.6			0.32		

II For  $\lambda = 0.4$

1.	0.2			0.08		
2.	0.4			0.16		
3.	0.6			0.24		
4.	0.8			0.32		
5.	1.0			0.40		
6.	1.2			0.48		



7. 1.4 0.56

8. 1.6 0.64

III For  $\lambda = 0.6$

1. 0.2 0.12

2. 0.4 0.24

3. 0.6 0.36

4. 0.8 0.48

5. 1.0 0.60

6. 1.2 0.72

7. 1.4 0.84

8. 1.6 0.96

IV For  $\lambda = 0.8$

1. 0.2 0.16

2. 0.4 0.32

3. 0.6 0.48

4. 0.8 0.64

5. 1.0 0.80

6. 1.2 0.96

7. 1.4 1.12

8. 1.6 1.28

V For  $\lambda = 1$

1. 0.2 0.2

2. 0.4 0.4

3. 0.6 0.6

4. 0.8 0.8

5.	1.0	1.0
6.	1.2	1.2
7.	1.4	1.4
8.	1.6	1.6

VI For  $\lambda = 1.2$

1.	0.2	.2.4
2.	0.4	.4.8
3.	0.6	.7.2
4.	0.8	.9.6
5.	1.0	.1.2
6.	1.2	1.44
7.	1.4	1.68
8.	1.6	1.92

VII For  $\lambda = 1.4$

1.	0.2	0.28
2.	0.4	0.56
3.	0.6	0.84
4.	0.8	1.12
5.	1.0	1.40
6.	1.2	1.68
7.	1.4	1.96
8.	1.6	2.24

VIII For  $\lambda = 1.6$

1.	0.2	0.32
----	-----	------

2. 0.4	0.64
3. 0.6	0.96
4. 0.8	1.28
5. 1.0	1.60
6. 1.2	1.92
7. 1.4	2.24
8. 1.6	2.56

### CONCLUSIONS;

From the graph plotted  $(v/a_t)_{M_0}$  vs  $(v/a_t)_{Pr}$  for various values of  $\lambda$ , we can interpolate  $(v/a_t)_{Pr}$  after finding the value of  $(v/a_t)_{M_0}$  on laboratory experiments. Even the intermediate values can be linearly interpolated. On observing the values of lead and copper as the target materials, it is advisable to go for lead as the material for model testing because the projectile velocities are small. These velocities can be achieved with much less expensive instruments and it will not be difficult task compared to that of copper. From the graphs drawn for the depth of penetration to impact velocities of model and as well as prototype. for a given depth of penetration we can find the corresponding impact velocities of projectiles in the case of model and as well as prototype.

In general for model experiments, it is preferable to go for a material in which the velocity of impact for a given depth of penetration is low because these velocities should be within the measurable capacity with ordinary expts, without much of instrumentation. The advantage of graphs of P/d vs velocities of penetration is irrespective of shape of the projectile. Once we determine the calibre or diameter we can find out the depth of penetration for a given velocity of impact or viceversa.

NOTE: The values of sound velocity of lead and copper are taken from "A Textbook of Chemistry and Physics" and also verified the values with the text of "Behaviour of Metals under impulsive loads" by Pearson.

### A4. Additional Calculations

As we have assumed, high carbon steel for the target material, the velocity of projectile impact in the case of prototype should be about 40,000 ft/sec.

We have the Eq. A 14 which reads:

$$\left(\frac{v}{a_t}\right)_{Pr} = \left(\frac{v}{a_t}\right)_{M_0} \frac{(\rho_p/\rho_t)_{M_0}}{(\rho_p/\rho_t)_{Pr}} \quad (A14)$$

Substituting a (V) = 40,000 ft/sec. we get

$$\left(\frac{40,000}{19,500}\right) = \left(\frac{V}{a_t}\right)_{M_0} \times 0.6877$$

$$\therefore (a_t)_{M_0} = 7086.96 \text{ ft/sec}$$

$$(V)_{M_0} = \left(\frac{40,000}{19,500.14}\right) \left(\frac{7086.96}{.6877}\right) = 21,138.94 \text{ ft/sec.}$$

As the model projectile velocity is very high, it is not a suitable material for laboratory testing of models, in order to test on the model, the velocity of sound on the material should be low, say around 2500ft/sec. The lesser the velocity, much will be the convenient to measure.

So firing the Model Projectile with velocity of 3000 ft/sec. we can calculate the velocity of sound in the model material and thereby chose the material accordingly. So, we have Equation (A 13)

$$\left(\frac{V}{a_t}\right)_{pr} = \left(\frac{V}{a_t}\right)_{M_0} \left(\frac{\rho_p}{\rho_t}\right)_{M_0} \quad (A13)$$

Choosing <sup>war</sup> as the model material we can calculate the velocity of model projectile made with copper.

For a prototype:

1. Assuming a projectile prototype velocity = 40,000 ft/sec.

We have

$$\left(\frac{40,000}{19,500.14}\right)_{pr} = \frac{V}{(1279.52)_{M_0}} \times \left(\frac{8.93}{.9}\right)_{M_0}$$

Hence,

$$V = 264 \text{ ft/sec.}$$

2. Assuming a projectile prototype velocity = 50,000 ft/sec.

$$\left(\frac{50,000}{19,500.14}\right)_{pr} = \left(\frac{V}{1279.82}\right) \times 9.92$$

Hence,

$$V = 330.72 \text{ ft/sec.}$$

$$3. \quad (V)_{M_0} = \frac{60,000}{19,500.14} \times \frac{1279.52}{9.92} = 395.59 \text{ ft/sec.}$$

$$4. \quad (V)_{M_0} = \frac{70,000}{19,500.14} \times \frac{1279.52}{9.92} = 463.015 \text{ ft/sec.}$$

$$5. \quad (V)_{M_0} = \quad \quad \quad = 529.16 \text{ ft/sec}$$

$$6. \quad (V)_{M_0} = \quad \quad \quad = 595.30 \text{ ft/sec.}$$

For a model:

Material of the target - wood (Elm)

Material for Projectile - Copper

Velocity of Sound in Elm = 3320 ft/sec.

For various values of projectile velocity of prototype, we can find the projectile velocity for model.

$$1. \quad V_{pr} = 40,000 \text{ ft/sec.}$$

$$V_{M_0} = 442.31 \text{ ft/sec.}$$

2. For 50,000 ft/sec.

$$V_{M_0} = 552.90 \text{ ft/sec.}$$

A ( )

A5. Calculation of size and penetration time of Projectile for prescribed depth of penetration

The maximum speed of impact expected is 4000 ft/sec.

The depth of penetration is given by Eq. A2

$$P/d = 2.755 \left( \frac{\rho_p v}{\rho_T a_T} \right)^{.63} \quad (A2)$$

where

P = depth of penetration

d = diameter of projectile

$\rho_p$  = density of projectile

$\rho_T$  = density of target

v = Impact velocity

$a_T$  = Bulk velocity of sound in target.

The dimensions of target are given in Fig. A8.

Since initial velocity of interface is know to be 3000 ft/sec. and the depth of penetration is 5/8", assuming uniform deceleration the required formula to calculate the time taken is given by:

$$t = \frac{2P}{v}$$
$$t = \frac{2 \times 5/8}{3000 \times 12} \text{ (sec)} = 34.72 \mu\text{sec.}$$

The actual time of penetration is longer and Force does not remain uniformly high.

The target material is aluminum and penetrator material is lead.

Density of lead ( $\rho_p$ ) = 2.7 gm/cc  
Density of Al ( $\rho_T$ ) = 11.35 gm/cc  
Speed of sound in Al ( $a_T$ ) = 20979 ft/sec.

Also

$v/a_T$  is given by

$$\frac{v}{a_T} = \frac{4000}{20979} = 0.191$$

This ratio is clearly much less than unity and cannot qualify as hypervelocity impact. Data extends into this region however.

Substituting the above values in (1) gives

$$\begin{aligned} \frac{P}{d} &= 2.755 (4.2 \times 1.91)^{.63} \\ &= 2.4 \end{aligned}$$

Assuming the maximum permissible depth of penetration to be 5/8", the diameter d is given by:

$$d = \frac{5/8}{2.4} = .26''$$

This value of diameter roughly checks with the caliber of the rifle used.

The stringent requirement that velocity of projectile has to surpass velocity of sound in target material is seldom met and has been found that the phenomena of penetration and crater formation is not significantly different even at velocities far below the speed of sound of target material.

A6. Calculations of a maximum force of impact

The corresponding speed in km/sec of the speed of impact of lead projectile is given by:

$$\begin{aligned} V (\text{km/s}) &= 4000 \text{ ft/sec} \times .000303 \text{ km/ft} \\ &= 1.212 \text{ km/sec} \end{aligned}$$

From the reflected Hugoniot the corresponding pressure is 0.2 megabar and interface velocity is 0.9 km/sec. or 3000 ft/sec.

Since diameter of projectile is .26" area of projectile assuming cylindrical shape is:

$$\begin{aligned} A &= \frac{\pi d^2}{4} = \frac{\pi \times .26^2}{4} \\ &= .0531 \text{ in}^2 \end{aligned}$$

The initial force exerted on target is :

$$\begin{aligned} F &= 0.2 \times 10^6 \times .0531 \text{ bar in}^2 \\ &= 0.2 \times 10^6 \times .053 \times 14.2 \\ &= 150520 \text{ lbf.} \end{aligned}$$



A7. Calculations of the supporting plate response

The force-time curve is assumed in the form shown in Fig. A9.

If maximum force is

$$F_{max} = 252000 \text{ lb} \quad , \quad \omega = \sqrt{\frac{k}{m}} = 950 \text{ rad/s}$$

$$T = 11 \mu\text{sec} \quad \quad m = \frac{2}{386} \cdot \frac{\text{lbs}^2}{\text{in}}$$

By convolution integral the deflection of the supporting place is

$$x = \frac{1}{m\omega} \int_0^T F(\xi) \sin \omega(t-\xi) d\xi \quad (A15)$$

The force at time will be

$$F = 25200 - \frac{252000}{11 \times 10^{-6}} \xi \quad (A16)$$

Substituting (A16) into (A17) and performing the required integration obtain

$$x = \frac{252000}{m\omega^2} (\cos(\omega(t-T)) - \cos \omega t)$$

$$- \frac{25200}{m\omega T} \left( \frac{T \cos(\omega(t-T))}{\omega} + \frac{\sin \omega(t-T) - \sin \omega t}{\omega^2} \right)$$

A program has been written to find  $x_{max}$  which turns out to be .283 in at time of  $1.7 \times 10^{-5}$  sec.

The force on support place

$$F_{plate} = 4666.7 \times .283 = 1322.1 \text{ lb.}$$

Table A1. Impact response of materials

$\dot{\epsilon}$	$V_s$	EFFECT	METHOD OF LOADING
$10^8$	$> 12 \text{ kms}^{-1}$	EXPLOSIVE IMPACT-COLLIDING SOLIDS VAPORIZED	—
$10^6$	$3-12 \text{ kms}^{-1}$	HYDRODYNAMIC-MATERIAL COMPRESSIBILITY NOT IGNOREABLE	EXPLOSIVE ACCELERATION
	$1-3 \text{ kms}^{-1}$	FLUID BEHAVIOR IN MATERIALS; PRESSURES APPROACH OR EXCEED MATERIAL STRENGTH; DENSITY A DOMINANT PARAMETER	POWDER GUNS, GAS GUNS
$10^4$	$500-1000 \text{ ms}^{-1}$	VISCOUS-MATERIAL STRENGTH STILL SIGNIFICANT	POWDER GUNS
$10^2$	$50-500 \text{ ms}^{-1}$	PRIMARILY PLASTIC	MECHANICAL DEVICES, COMPRESSED AIR GUN
$10^0$	$< 50 \text{ ms}^{-1}$	PRIMARILY ELASTIC SOME LOCAL PLASTICITY	MECHANICAL DEVICES, COMPRESSED AIR GUN
0			

Table A2. RELEVANT PROPS FOR HIGH SPEED IMPACT  
FOR 5 MATERIALS

Material	n(Latent heat: of fusion)	$t_m$ °C (Melting Pt)	P (gm/cc)	C (cal / gm/ °C).	Speed of Sound bulk ft/s
Aluminum	95.0	660	2.7	0.215	209.79, 17200
Copper	42.0	1084	8.96	0.092	15734 11750
Lead	5.5	327.5	11.35	0.031	7080 4100
Steel	65	1515	7.86	0.107	19986 <sup>1</sup> 16,600
Wax	42.3	61.8	0.96		4917

Source: Handbook of Tables for Applied Engineering Science

Table A3.

II TERM RATIOS, PROTOTYPE: LEAD PEN, STEEL TARGET

Copper Target	$\pi_6^m / \pi_6^p$	$\pi_{15}^m / \pi_{15}^p$	$\pi_{11}^m / \pi_{11}^p$	$\pi_{12}^m / \pi_{12}^p$	$\pi_{13}^m / \pi_{13}^p$
Tin Pen	0.565	0.950	1.921	4.000	1.464
Copp. Pen	0.693	0.950	4.634	11.820	3.448
Al. Pen	0.208	0.950	2.819	26.736	8.066
Lead Pen	0.876	0.950	1.395	1.536	1.162
Steel Pen	0.609	0.950	6.435	18.300	4.024
Zinc Pen	0.540	0.950	3.36	7.588	3.489
Al Target					
Lead Pen	2.920	0.600	2.315	0.680	0.500
Al Pen	.700	0.600	4.63	11.82	3.45
Copp. Pen	2.300	0.600	7.600	5.22	1.481
Steel Pen	2.00	0.600	10.660	8.274	1.717
Tin Pen	1.875	0.600	3.240	1.754	0.626
Zinc Pen	1.800	0.600	4.612	3.360	1.500
Wax Target					
Zinc Pen	5.055	0.292	59.013	7.54	0.644
Tin Pen	5.273	0.292	33.735	3.940	0.250
Lead Pen	8.188	0.292	62.530	11.736	0.637
Copp. Pen	6.46	0.292	81.279	11.903	18.8
Al Pen	1.048	0.292	49.486	26.546	1.484

Lead Target/Al Pen	0.165	0.740	9.268	204	24.00
Copp Pen	0.546	0.740	15.361	90.189	10.24
Lead Pen	0.692	0.740	4.634	11.82	3.460
Steel Pen	5.443	0.740	21.549	139.692	11.91
Tin Pen	0.446	0.740	6.372	30.26	4.31
Zinc Pen	0.426	0.740	11.163	58.038	10.355

Table, A4 Results of Calculations for Model and Prototype.

Material of the Model: Target material - lead.  
Projectile: High carbon steel

Material of the Prototype: Target: High Carbon Steel  
Projectile: High Carbon

Ser. No.	Depth of Penetration P/d	Velocity of Projectile for Model ft/sec.	Velocity of Projectile for Prototype ft/sec.
1.	0.2	189.57	348.48
2.	0.4	535.81	1013.27
3.	0.6	985.09	1862.97
4.	0.8	1516.65	2868.17
5.	1.0	2119.30	4007.40
6.	1.2	2786.27	5268.59
7.	1.4	3511.10	6639.68

Table A5: Results of calculations for a model and prototype

Material of the Model: Target: Material copper.  
Projectile: High Carbon Steel.

Material of the Prototype: Target material: High Carbon Steel  
Projectile: High Carbon Steel

Ser. No.	Depth of Penetration P/d	Velocity of Projectile in Model ft/sec.	Velocity of Projectile in Prototype ft/sec.
1.	0.2	327.32	3576.37
2.	0.4	921.44	1009.58
3.	0.6	1702.31	1865.19
4.	0.8	2618.59	2874.73
5.	1.0	3659.56	4004.08
6.	1.2	4810.52	5270.33
7.	1.4	6062.11	6682.99

Table A6: Results of Calculations for Model and Prototype

Material of Model: Target: Wood (Elm)  
Projectile: copper

Material of Prototype Target: High Carbon Steel  
Projectile: High Carbon Steel

Ser. No.	Velocity of Prototype Projectile. ft/sec.	Velocity of Model Projectile. ft/sec.
1.	40,000	442.31
2.	50,000	552.90
3.	60,000	663.47
4.	70,000	774.05
5.	80,000	884.62
6.	90,000	995.20



Table A7: Results of Calculations for Model and Prototype

Material of Model:

Target: Wax  
Projectile: Copper

Material of Prototype:

Target: High Carbon Steel  
Projectile: High Carbon Steel

Speed of sound in wax - 1279.52 ft/sec.

Density of Wax - 0.9 gm/cc.

Density of Copper - 8.93 gm/cc.

Ser. No.	Prototype of Projectile ft/sec.	Model of Projectile Velocity ft/sec.
1.	40,000	264
2.	50,000	330.72
3.	60,000	395.59
4.	70,000	463.01
5.	80,000	529.16
6.	90,000	595.30

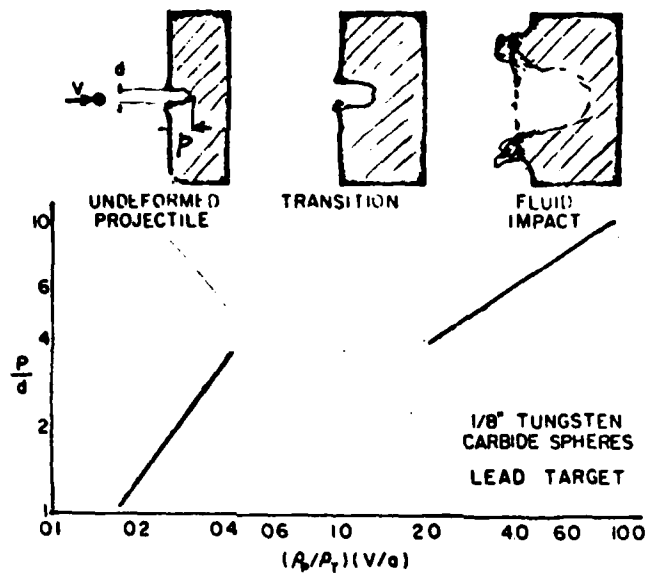


Figure A1. Basic Types of Impact (Ref. 2).

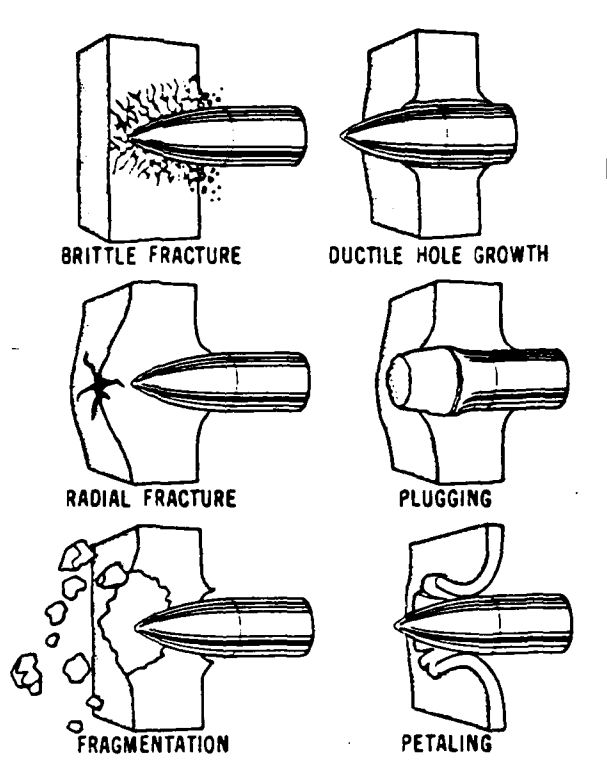


Figure A2. Failure modes in impacted plates. Ref 1

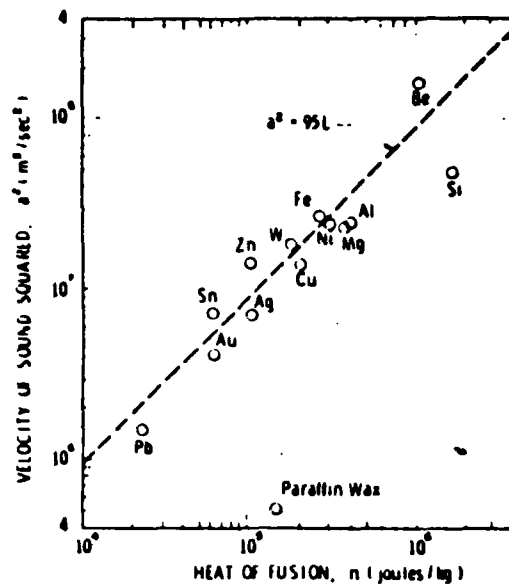


Figure A3. Velocity of Sound Squared versus Heat of Fusion for Various Materials (Ref. 7).

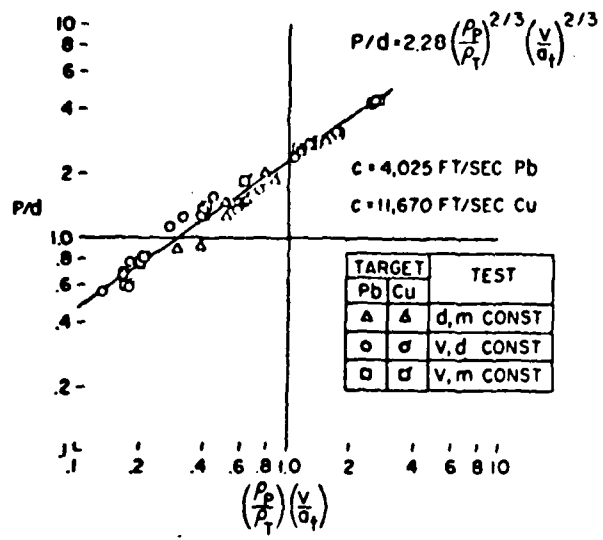


Figure A4. Penetration versus Impact Parameter (Ref. 2 ).

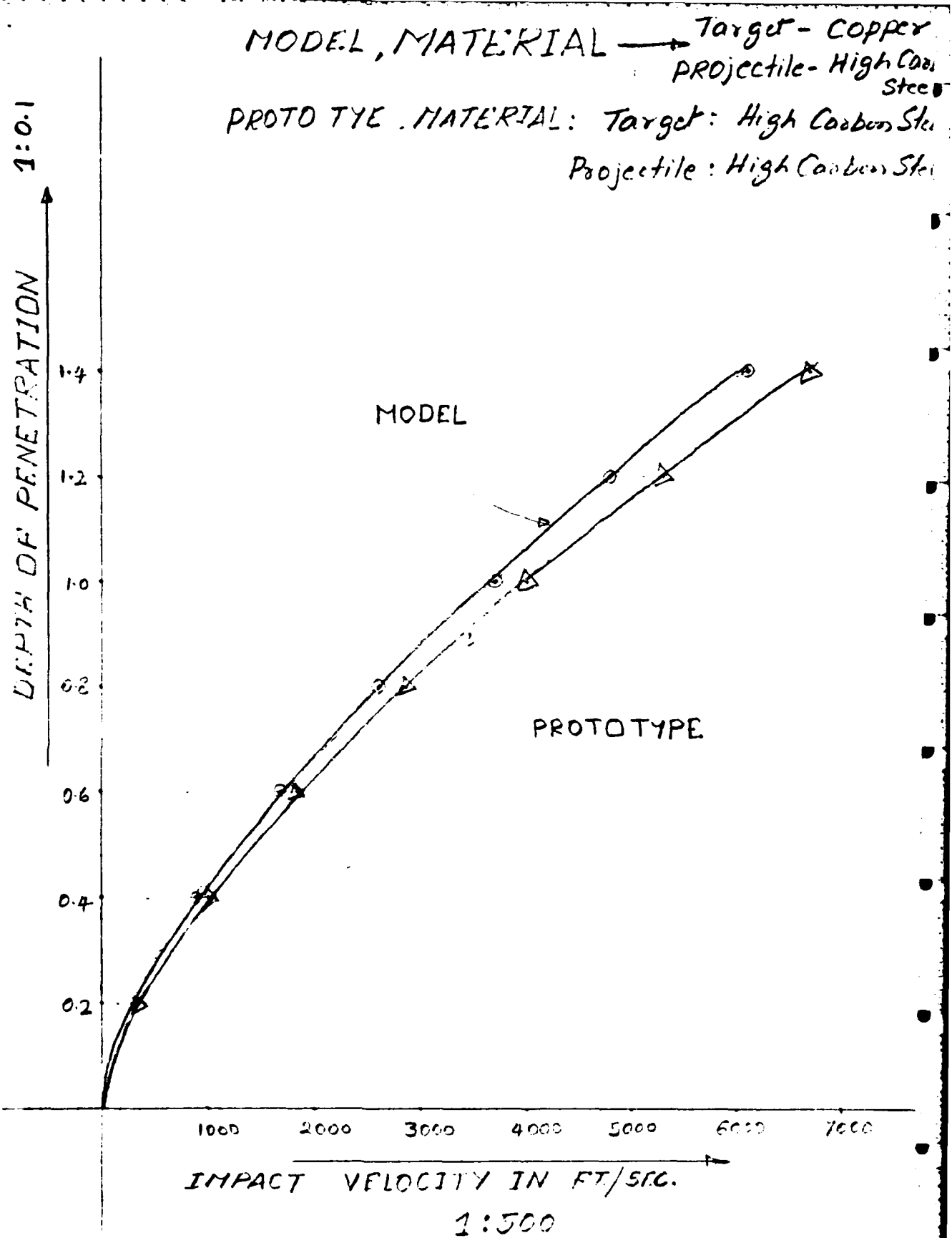


Fig. A5. Effect of impact velocity on the depth of penetration.

MATERIAL OF MODEL : Target - Lead  
Projectile - High Carbon Steel

MATERIAL OF PROTOTYPE : Target - High Carbon Steel  
Projectile - High Carbon Steel

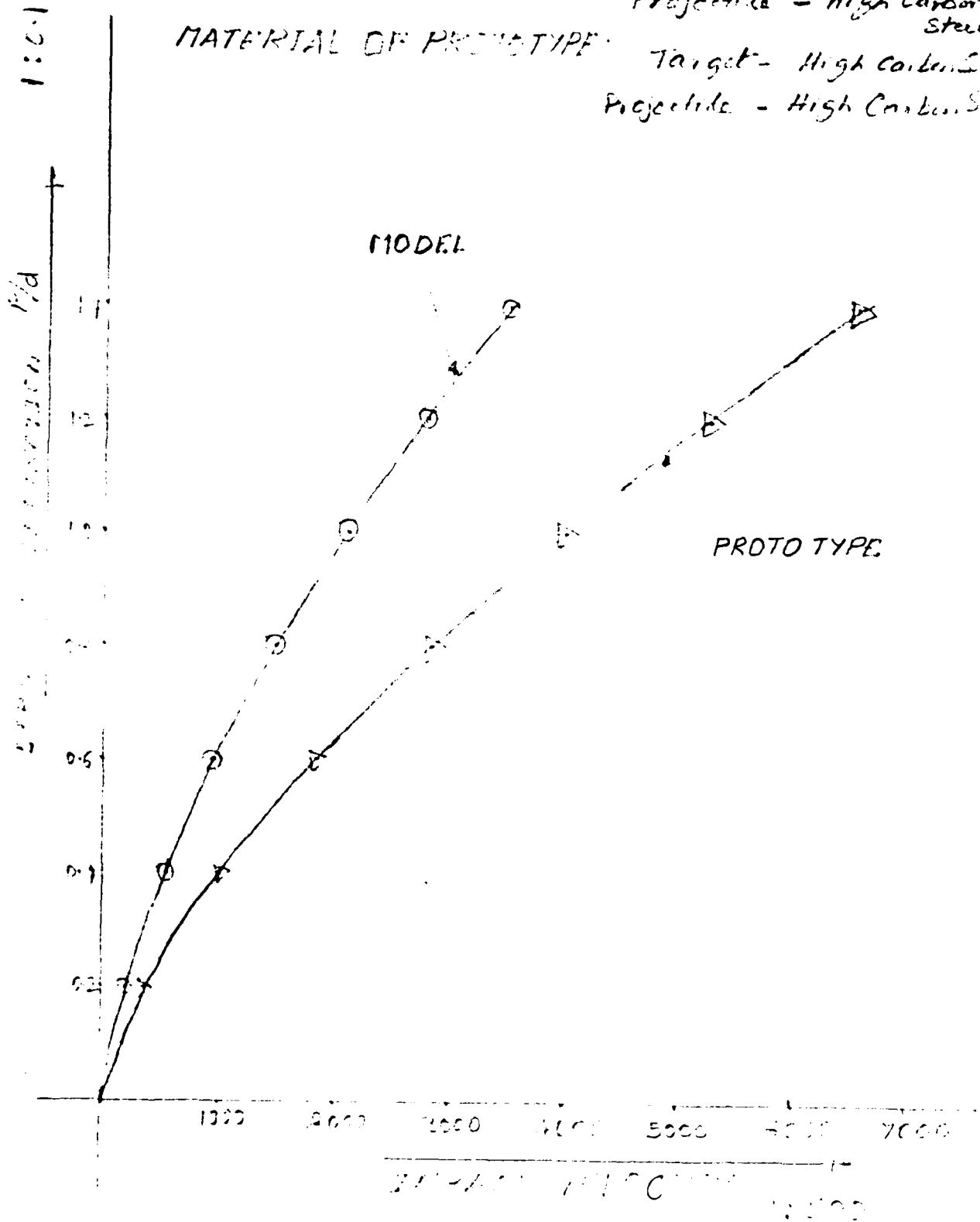


Fig. A6. Effect of impact velocity on the depth of penetration

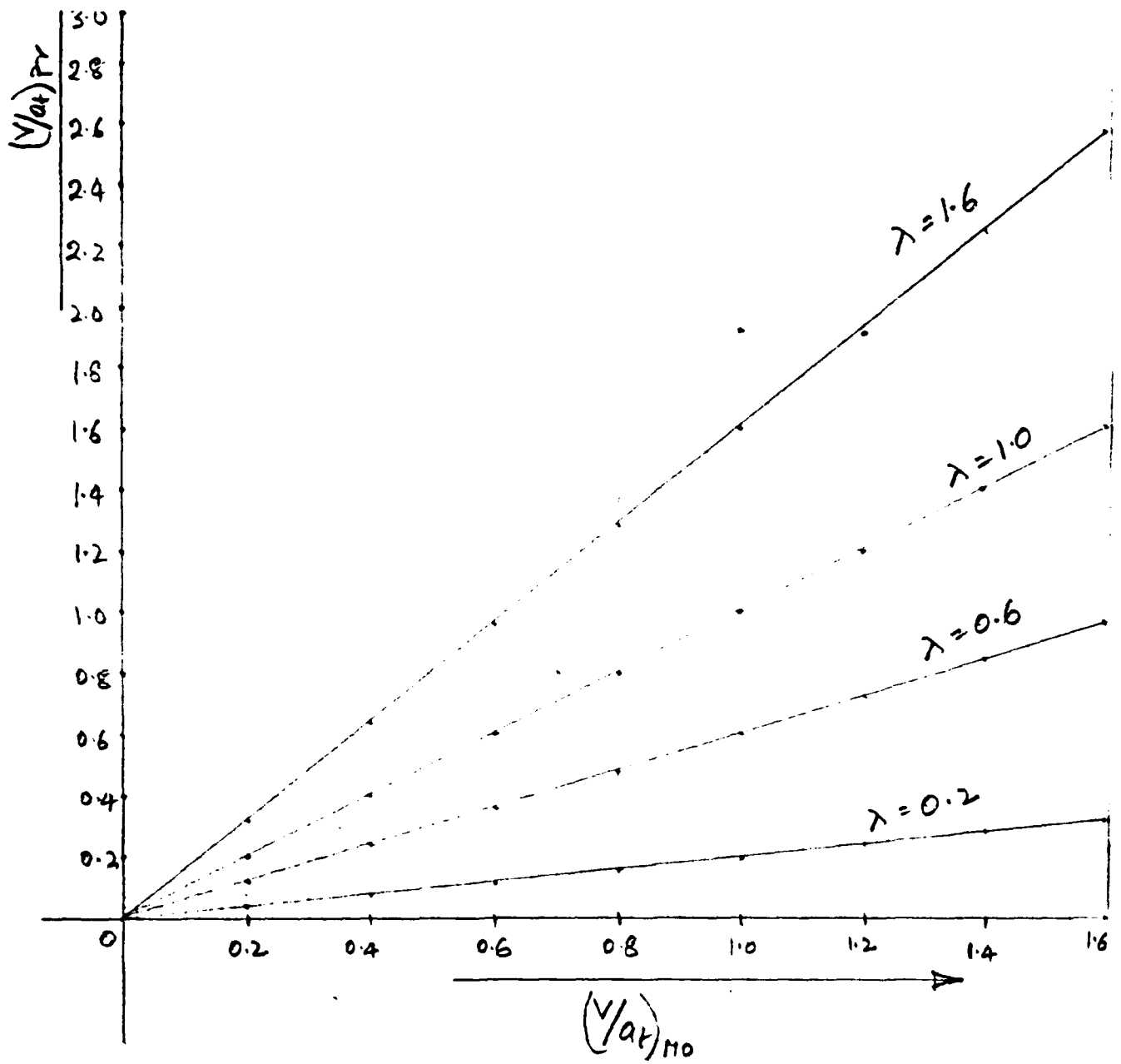


Fig. A7. Effect of impact velocity on the depth of penetration.



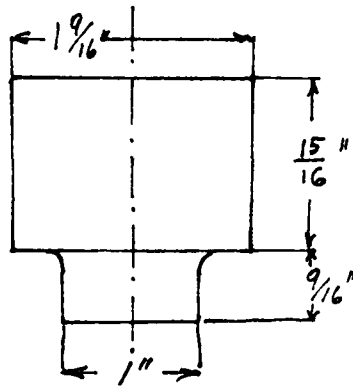


Fig. A8. Al. target with dimensions

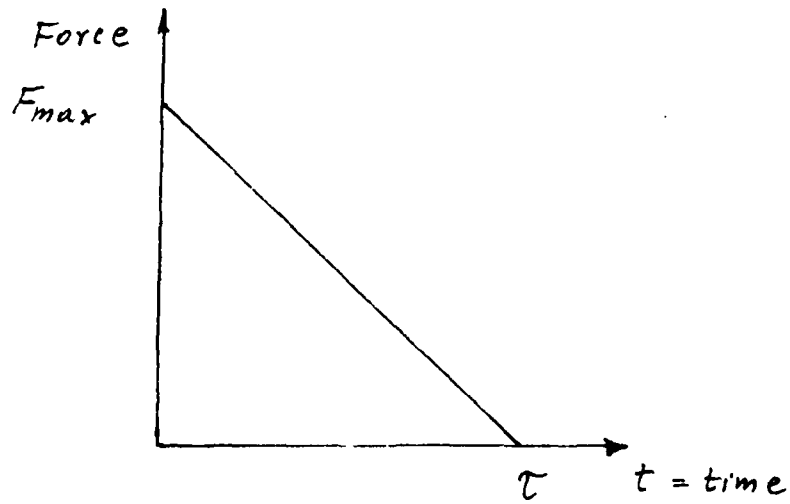


Fig. A9. The force-time curve assumed for a preliminary calculation.

APPENDIX B  
EXPERIMENTAL DETERMINATION OF THE PENETRATION FORCE

Consider a model for the striker and armour as shown in Figure B1. Mass of a striker is  $M_1$  and mass of an armour is  $M_2$ . If the instantaneous positions of center of mass of a striker  $O_1$  and armour  $O_2$  with respect to the reference lines are  $Z_1(t)$  and  $Z_2(t)$  respectively and spring constant of the supporting spring is  $k$ . The two following equations hold

$$m_1 \ddot{z}_1(t) = -F_p(\alpha) \quad (B1)$$

$$m_2 \ddot{z}_2(t) = F_p(\alpha) - k z_2(t) \quad (B2)$$

where:

$$\alpha = z_1 - z_2 \quad \text{and}$$

$$F_p(\alpha) = \text{penetration force at}$$

this instant ( $\alpha$ ) or  $t$

Integrating Eq (B2) gives:

$$\dot{z}_2 \Big|_{t=T} = \frac{1}{m_2} \int_0^T F_p(t) \cos \omega_n (T-t) dt \quad (B3)$$

$$z_2 \Big|_{t=T} = \frac{1}{m_2 \omega_n} \int_0^T F_p(t) \sin \omega_n (T-t) dt \quad (B4)$$

where  $\omega_n = \sqrt{\frac{k}{m_2}}$  is the natural frequencies of the armour plate on the spring  $k$ .

If the armour is free to move ( $k = 0$ ) the velocity and displacement will be

$$\dot{z}_2 \Big|_{t=T} = \frac{1}{m_2} \int_0^T F_p(t) dt \quad (B5)$$

$$z_2 \Big|_{t=T} = \frac{1}{m_2} \int_0^T F_p(t) (T-t) dt \quad (B6)$$

By comparison Eq. (B5) and (B6) with Eqs. (B3) and (B4) we conclude that the difference between relative velocities and displacements in both cases is less for smaller value of

If  $\omega_n T < \frac{\pi}{10}$  or the period of free oscillations is at least 20 times larger than the time of penetration. The error in velocity is less than 5% and the error in displacement is less than 2%. In

conclusion the support stiffness  $k$  may be neglected.

With this assumptions the test force transducers are designed to be used in this research.

Neglecting the second term on r.h.s. of Eq.(B2), multiplying Eq.(B1) by  $M_2$  and Eq. (B2) by  $m_1$  and adding, gives:

$$m_1 m_2 \ddot{\alpha} = -(m_1 + m_2) F_p(\alpha)$$

or

$$\ddot{\alpha} = - \frac{F_p(\alpha)}{m} \quad (B7)$$

where:

$$m = \frac{m_1 m_2}{m_1 + m_2}$$

and  $\alpha = Z_1 - Z_2$  is called the "approach." The first integral of Eq. (B7) will be

$$\frac{1}{2} \left( \frac{d\alpha}{dt} \right)^2 = - \frac{1}{m} \int_0^{\alpha} F_p(\alpha) d\alpha + C \quad (B8)$$

since for  $t = 0$ ,  $\alpha = 0$  and  $\frac{d\alpha}{dt} = V_0$ , the integration constant  $C$  is equal  $V_0^2/2$  so

$$\left( \frac{d\alpha}{dt} \right)^2 - V_0^2 = - \frac{2}{m} \int_0^{\alpha} F(\alpha) d\alpha \quad (B9)$$

The approach  $\alpha$  becomes a maximum if  $\frac{d\alpha}{dt} = 0$  and its value can be determined from equation:

$$\frac{2}{m} \int_0^{\alpha_{max}} F_p(\alpha) d\alpha = V_0^2 \quad (B10)$$

Actually this value of a maximum approach  $\alpha_{max}$  can be measured from the experiment and it is equal to the depth of penetration. Hence, the penetration force  $F_p$  is determined from Eq. (B10). For this purpose we assume

$$F_p(\alpha) = g \alpha^n \quad (B11)$$

where:  $g$  and  $n$  will be determined from the experiment.

Substituting Eq. (B11) for B(10) and performing source algebra gives

$$\alpha_{max}^{n+1} = (n+1) \frac{m V_0^2}{2g} \quad (B12)$$

The total time of the impact  $T_{imp}$  is calculated directly from Eq.(B9) as

$$T_{imp} = \int_0^{\alpha_{max}} \frac{d\alpha}{\sqrt{V_0^2 - \frac{2}{m} \int_0^{\alpha} F_p(\alpha) d\alpha}} \quad (B13)$$

Substituting

$$\int_0^{\alpha} F_p(\alpha) d\alpha = q \int_0^{\alpha} \alpha^n d\alpha = q \frac{\alpha^{n+1}}{n+1}$$

into Eq. (13) gives

$$T_{imp} = \int_0^{\alpha_{max}} \frac{d\alpha}{\sqrt{V_0^2 - \frac{2q}{(n+1)m} \alpha^{n+1}}} \quad (B14)$$

Equations (B12) and (B14) can now be solved simultaneously for  $q$  and  $n$ .

From Eq. (B12)

$$2q = \frac{(n+1) m V_0^2}{\alpha_{max}^{n+1}} \quad (B15)$$

substituting Eq. (B15) into Eq. (B14) gives

$$T_{imp} = \int_0^{\alpha_{max}} \frac{d\alpha}{\sqrt{V_0^2 - \frac{(n+1) m V_0^2}{m \alpha_{max}^{n+1} (n+1)}}}$$

or

$$T_{imp} = \frac{1}{V_0} \int_0^{\alpha_{max}} \frac{d\alpha}{\sqrt{1 - \left(\frac{\alpha}{\alpha_{max}}\right)^{n+1}}} \quad (B16)$$

$$\text{if } \frac{\alpha}{\alpha_{\max}} = f$$

$$d\alpha = \alpha_{\max} df$$

so

$$T_{\text{imp}} = \frac{\alpha_{\max}}{V_0} \int_0^1 \frac{df}{\sqrt{1-f^{(n+1)}}} \quad (\text{B17})$$

or

$$\frac{V_0 T_{\text{imp}}}{\alpha_{\max}} = \int_0^1 \frac{df}{\sqrt{1-f^{(n+1)}}} = G \quad (\text{B18})$$

The values of G for various values of n were calculated and plotted in Figure B2.

## Sample Calculations

If the impact velocity  $V_0 = 4000 \text{ ft/sec}$   
 mass of the striker  $m_1 = .1 \text{ oz}$   
 mass of the armour  $m_2 = 16 \text{ oz}$   
 penetration depth  $\alpha_{\text{max}} = 1 \text{ in}$

From Eq (B18)

$$G = 1.55 = \frac{4000 \times T_{\text{imp}}}{1}$$

and  $T_{\text{imp}} = .0003875$

for  $n = .4$        $n+1 = 1.4$

$$Q = \frac{(n+1) m V_0^2}{2 \alpha_{\text{max}}^{(n+1)}}$$

$$m = \frac{m_1 m_2}{m_1 + m_2} = \frac{.1 \times 16}{16.1 \times 32} = .00311$$

$$Q = \frac{1.4 \times .00311 \times 4000^2}{2 \times 1} = 34832 \text{ lb}$$

$$F_p = Q \alpha^n = 34832 \alpha^{.4}$$

hence the maximum penetration force

$$F_{p_{\text{max}}} = 34832 \text{ lbs}$$

The maximum displacement is calculated from the conservation of momentum of the mass centers

$$x_{2_{\text{max}}} = \frac{m_1}{m_1 + m_2} V_0 T = \frac{.1}{16.1} \times 4000 \times .0003875$$

$$= .0962 \text{ in}$$

$$T_0 = 20T = 20 \times .0003875 = .00775, \rightarrow R = \frac{4\pi^2 \times 16.1}{384 \times .00775}$$

$$= 216.6 \text{ lb/in, Force in the spring} = 216.6 \times .0962 = 20.5 \text{ lb}$$

Table B1

RELEVANT PROPS FOR HIGH SPEED IMPACTFOR 5 MATERIALS

MATERIAL	n (Latent heat of fusion)	$0^{\circ}\text{C}$ (Melting $P_t$ )	(gm/cc)	C (Cal. 1 gm/ $^{\circ}\text{C}$ )	Speed of Sound ft/s (bulk)	(bar)
Aluminum	95.0	660	2.7	0.215	209.79	17200
Copper	42.0	1084	8.96	0.092	15734	11750
Lead	5.5	327.5	11.35	0.031	7080	4100
Steel	65	1515	7.86	0.107	19486	16600
Wax	42.3	61.8	0.96		4917	

Source: Handbook of Tables for Applied Engineering Science.



TABLE B2 TERM RATIOS, PROTOTYPE: LEAD PEN. STEEL TARGET

Copper Target

Tin Pen.	0.565	0.950	1.921	4.000	1.434
Copp. Pen	0.693	0.950	4.634	11.820	3.448
Al. Pen.	0.208	0.960	2.819	26.736	8.066
Lead Pen.	0.876	0.950	1.395	1.536	1.162
Steel Pen.	0.609	0.950	6.435	18,300	4.024
Zinc Pen.	0.540	0.950	3.36	7.588	3.489

Al Target

Lead Pen.	2.920	0.600	2.315	0.680	0.500
Al Pen.	.700	0.600	4.63	11.82	3.45
Copp. Pen.	2.300	0.600	7.600	5.22	1.481
Steel Pen.	2.00	0.600	10.660	8.274	1.717
Tin Pen	1.875	0.600	3.240	1.754	0.626
Zinc Pen.	1,800	0.600	4.612	3.860	1.500

Wax Target

Zinc Pen.	5.055	0.292	59.013	7.54	0.644
Tin Pen.	5.273	0.292	33.735	3.940	0.250
Lead Pen.	8.188	0.292	62.530	11.736	0.637
Copp. Pen.	6.46	0.292	81.279	11.903	18.8
Al. Pen.	1.948	0.292	49.486	26.546	1.484

Lead Target/Al Pen

Lead Target/Al Pen	0.165	0.740	9.268	204	24.00
Copp. Pen	0.546	0.740	15.361	90.189	10.24
Lead Pen.	0.692	0.740	4.634	11.82	3.460
Steel Pen.	5.443	0.740	21.549	139.692	11.91
Tin Pen.	0.446	0.740	6.372	30.26	4.31
Zinc Pen.	0.426	0.740	11.163	58.038	10.355

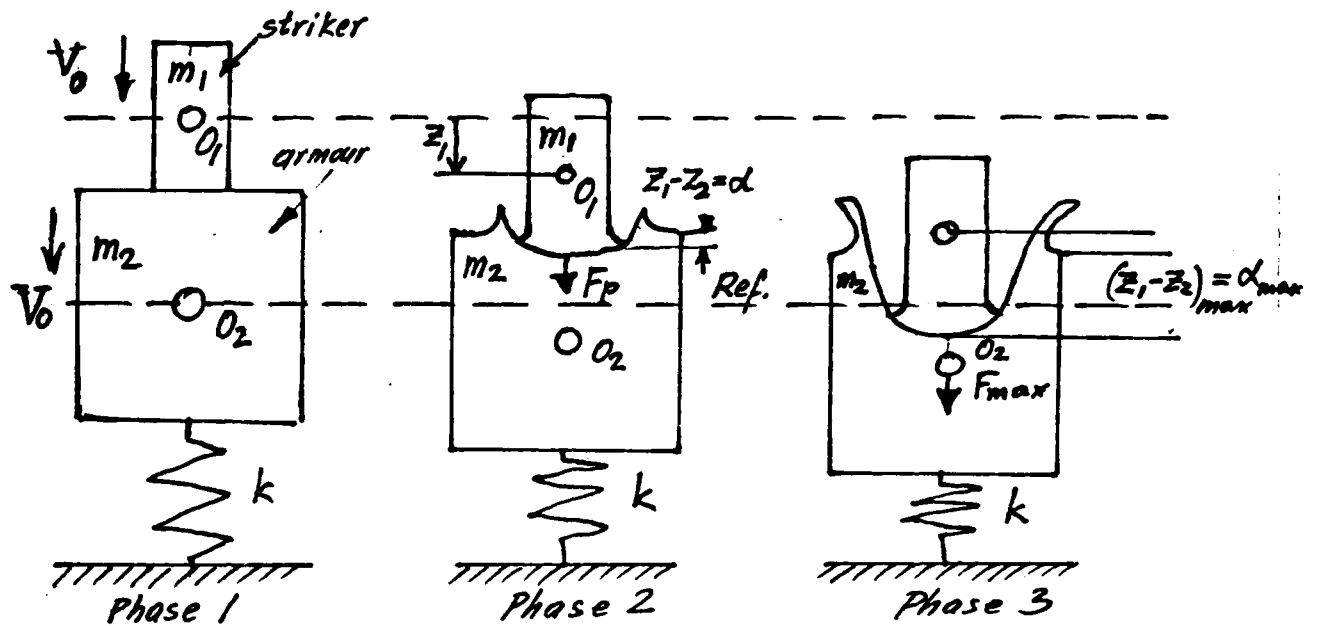


Fig. B1. Schematic representation of the impact between striker and armour material. Displacements of the mass centers of the striker  $O_1$  and armour  $O_2$  are referred to position at the first contact instant.  $F_p$  is the penetration force.

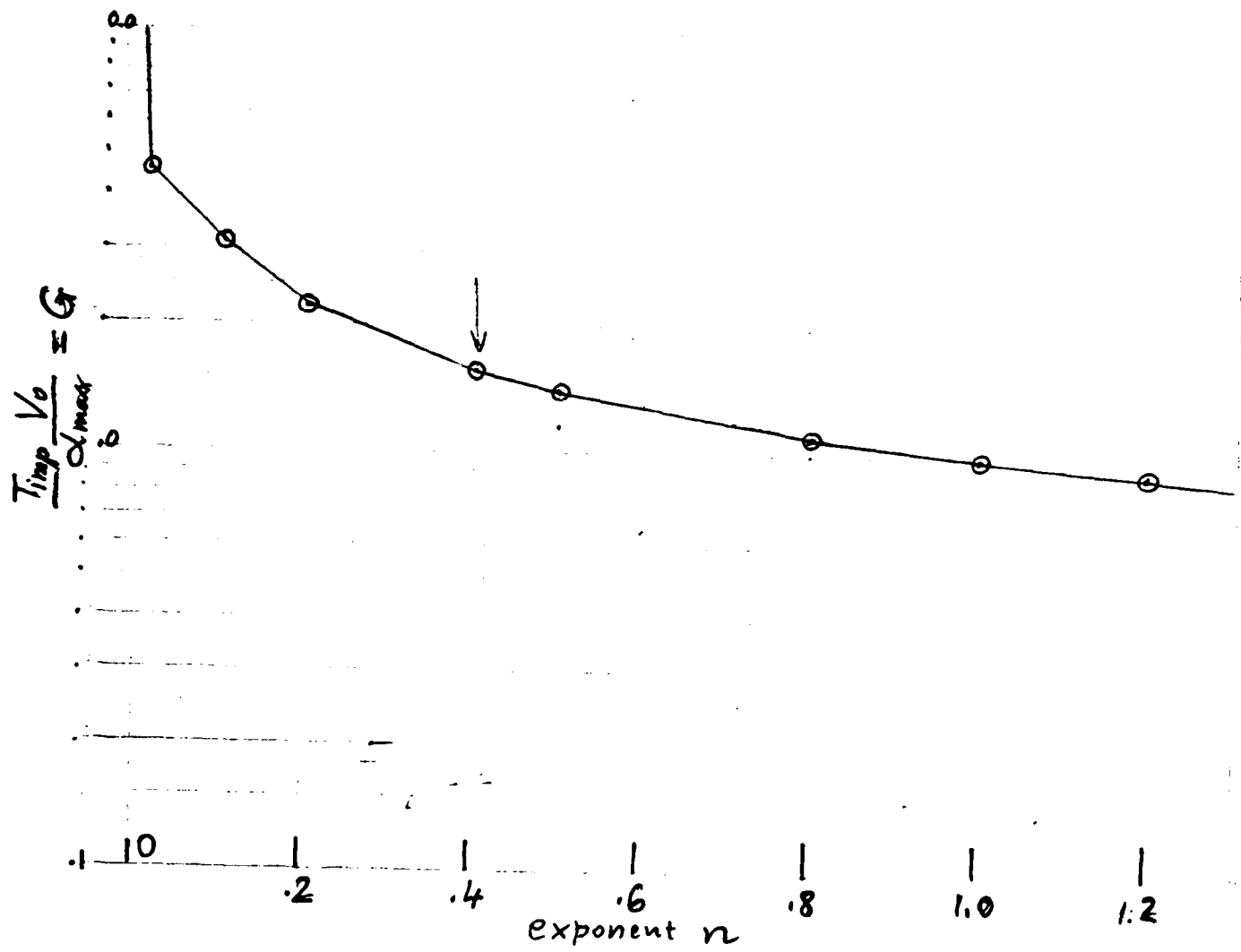
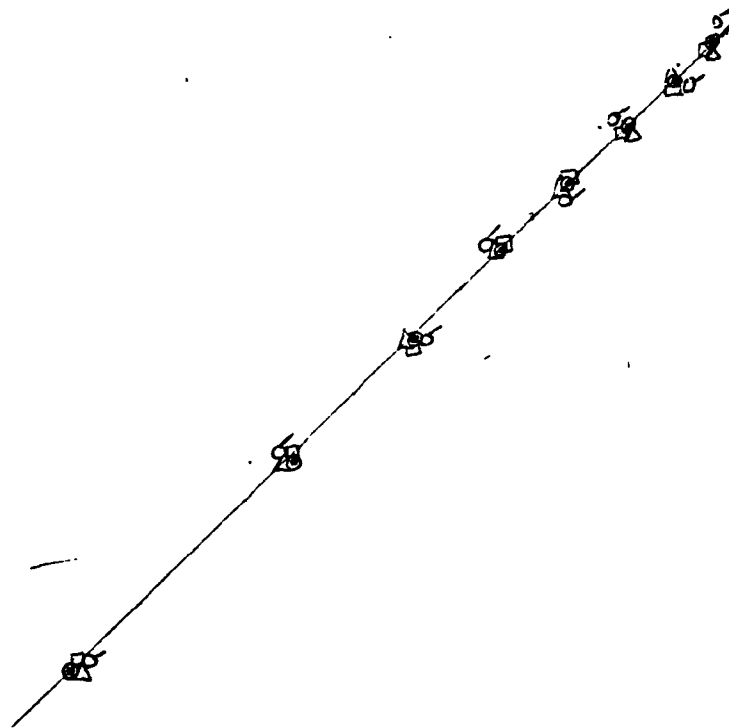


Fig. B2. Graph of the function G

$$P/D = \frac{\text{penetration}}{\text{diameter}}$$



- ⊙ Aluminium
- △ Copper
- Steel
- ⊖ Lead

$$\left(\frac{P_P}{P_T}\right)\left(\frac{V}{a_t}\right)$$

Fig. B3. Penetration vs impact parameter.

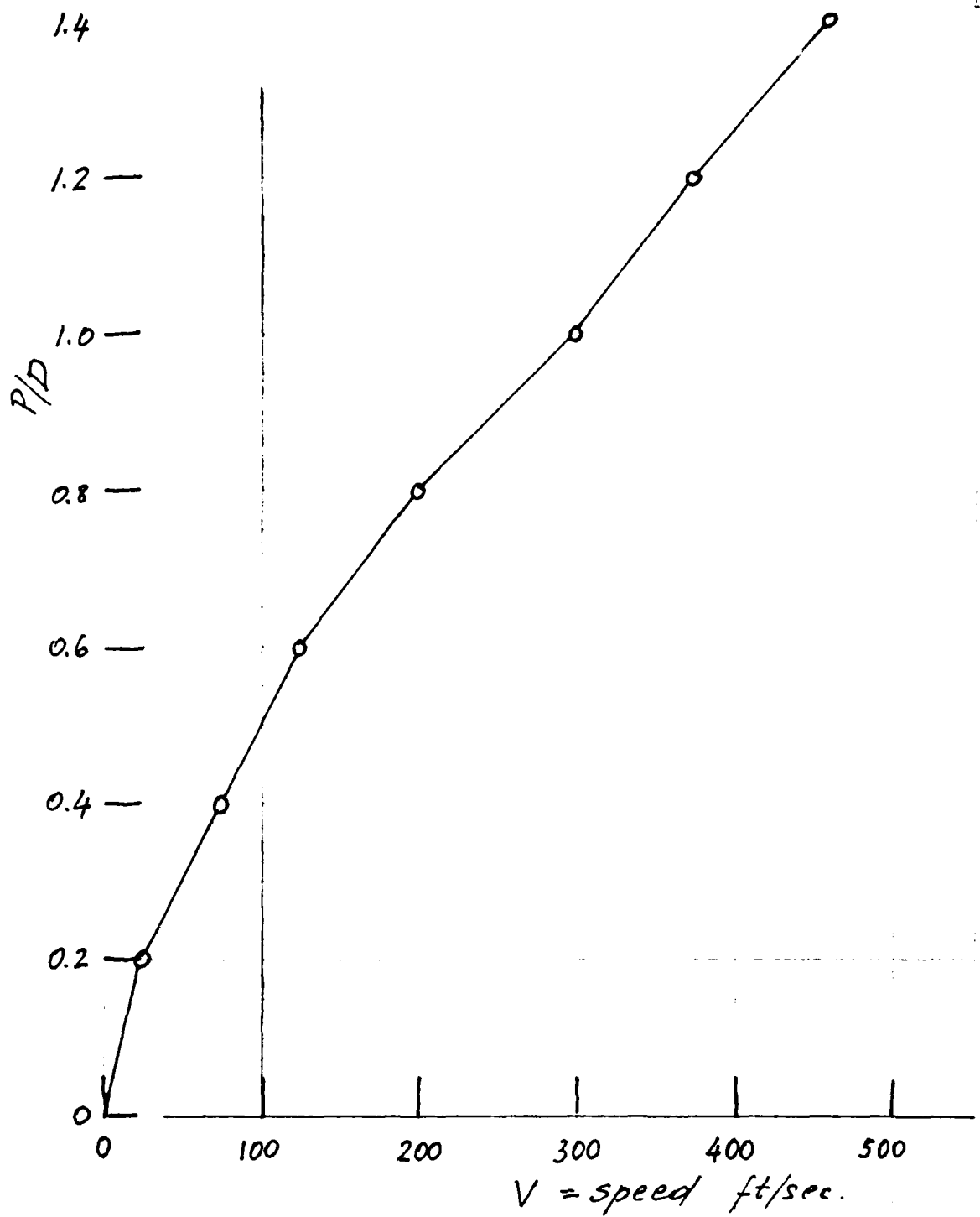


Fig. B4. Speed of a lead penetrator and penetration for a wax target

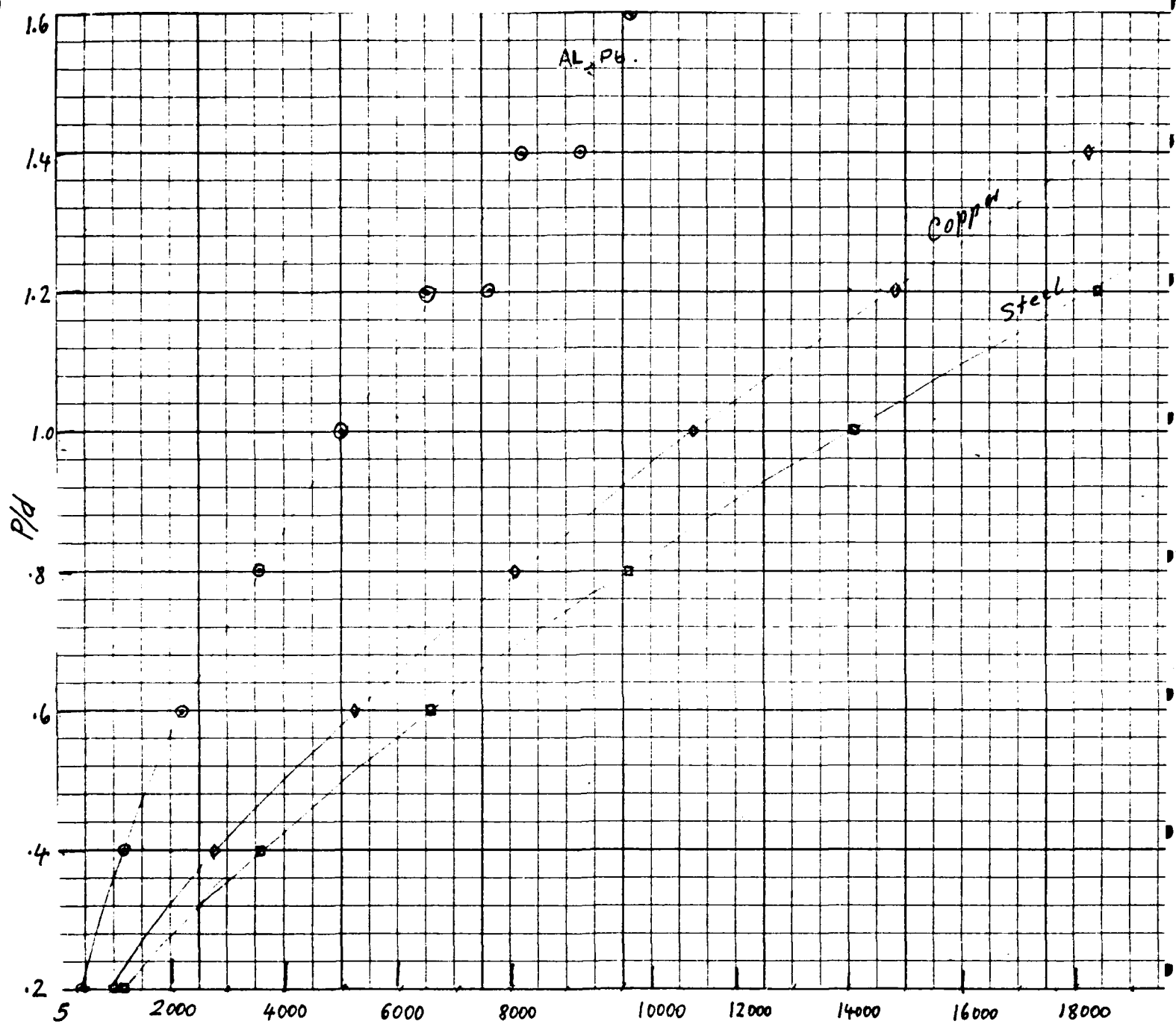


Fig. B5 Effect of the impact velocity on the depth of penetration for Lead, Aluminum, Copper and Steel with the lead penetrator.

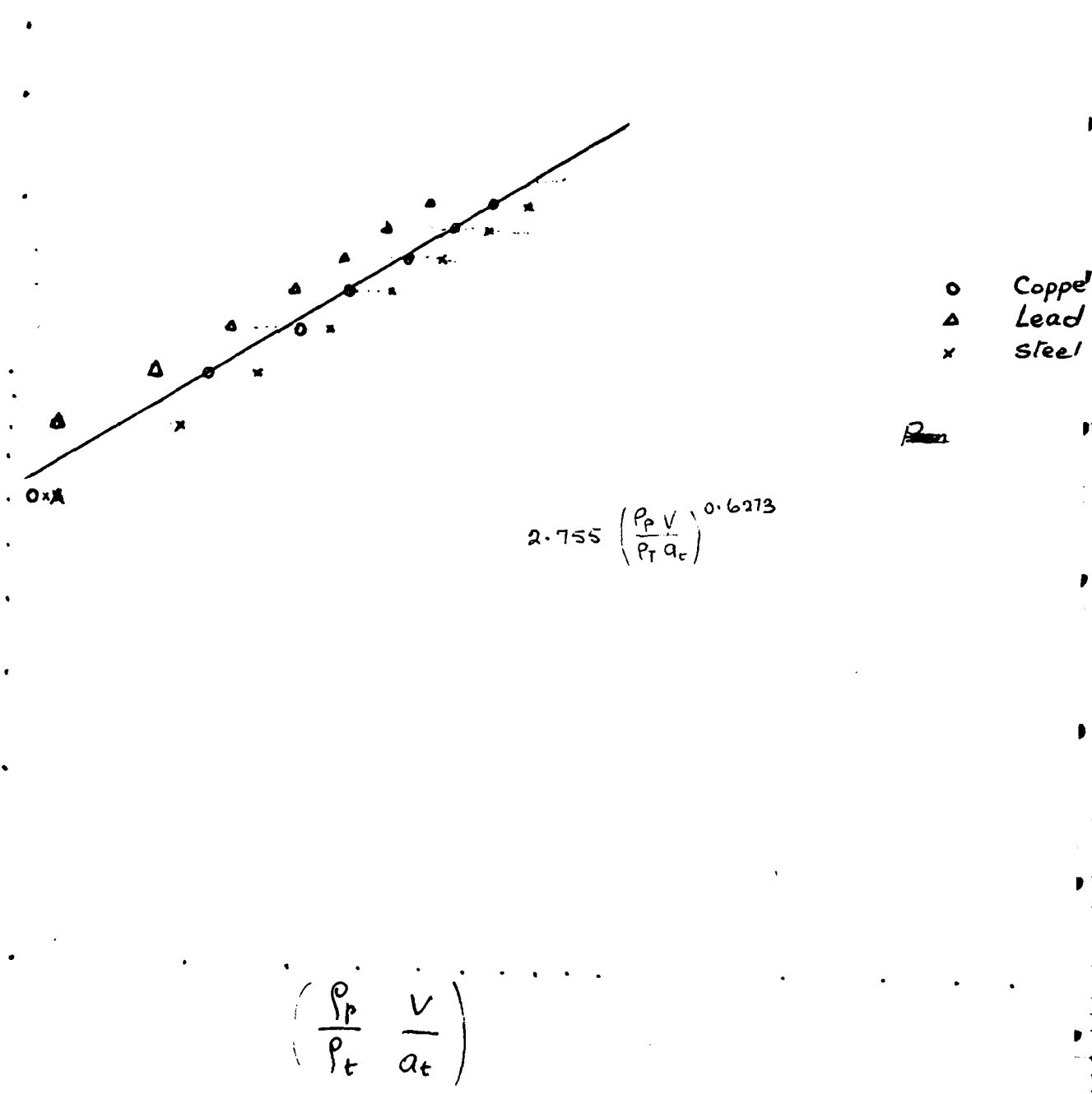


Fig. B6. Penetration versus impact parameters with a speed of sound being bulk velocity.

APPENDIX C  
DESIGN OF IMPACT FORCE TRANSDUCERS

Two types of transducers have been taken into consideration for effective use in the test. 1. Membrane transducer, 2. Beam transducer (single and double beam). Each has got its own merits and demerits.

C1. Membrane Transducer

(a) Since it is circular one and clamped around by flanges even for eccentric load more accurate response is assured.

(b) Since a hole is present at the center of the membrane in which a plug with specimen rests it is possible to perform the test on piercing also.

(c) The membrane has a limited space to mount strain gages.

(d) It is not easily accessible from the bottom.

C2. Beam Transducer

(a) This beam can't be used for test of piercing type. Only usable with penetration tests.

(b) It has got more room to mount gages both on top and bottom of the beam.

(c) Easy accessibility comparing membrane transducer.

(d) Since beam is of 24" span the response for load is high with strain gages comparing the membrane transducer.

The membrane transducer consists of a circular membrane of 5 5/16" diameter carbon steel plate of 1/16" thickness and with a 1" hole as shown in figure C1. The target material to be tested is supported by a plug that goes into the hole and rests on the membrane through the knife edge on the plug circumference. This membrane is clamped by two flanges which are bolted together keeping the membrane in between as shown in Figure C2. The two flanges are in turn, supported by a pipe of 6" diameter and about 3' long and the pipe rests on an aluminum plate of thickness 1" as shown in Figure C4.

The plug over which the sample has to sit is made of aluminum and this sits over the membrane through the knife edge as shown in the Figure C3.

The membrane is clamped around to get good axial response and to minimize the friction at support.

To measure the axial response of the membrane for the impact force strain gages are fixed to the top surface of the membrane as shown in figure C5. Two rosette strain gages and two ordinary strain gages are fixed on the membrane at 90° to each other. the rosette gage



is fixed at a radius of 2 1/2" in such a way to get the radial response, transverse response and also the response at 45° to the radial line. The strain gages that are fixed to the membrane is of 120 resistance and of paper back type. The leads from the gages are soldered to the terminals T55 from which in turn lead wires go to balancing bridges or to the leads of the Q plug in unit of oscilloscope.

### C3. Stress calculations in the membrane transducer

The flat plate whose stiffness is to be determined is to be used to support targets in an experiment on impact. Since the displacements of the plate can be used to determine the force acting on the plate the stiffness has to be determined. Also the maximum stress in the plate has to be kept within safe limits. Given a certain force of impact the maximum stress and stiffness depend on the location of the loads on the plate and plate dimensions. The mode of loading is shown in Figure (C6).

The max deflection  $y_{max}$ , radial stress  $S_r$ , and tangential stress are calculated by means of the following formulas taken from Reference 5.

$$y_{max} = - \frac{3W(m^2-1)}{4\pi m^2 E b^3} \left\{ a^2 - b^2 + \frac{2mb^2(a^2-b^2) - 8ma^2b^2 \log \frac{a}{b} + 4a^2b^2(m+1) \left(\log \frac{a}{b}\right)^2}{a^2(m-1) + b^2(m+1)} \right\} \quad (C1)$$

$$S_r = \frac{3W}{2\pi t^2} \left[ 1 - \frac{2mb^2 - 2b^2(m+1) \log \frac{a}{b}}{a^2(m-1) + b^2(m+1)} \right], \quad S_t = S_{max} \text{ if } \frac{a}{b} < 2.4 \quad (C2)$$

$$S_t = \frac{3W}{2\pi m t^2} \left[ 1 + \frac{ma^2(m-1) - mb^2(m+1) - 2(m^2-1)a^2 \log \frac{a}{b}}{a^2(m-1) + b^2(m+1)} \right]$$

$$S_t = S_{max} \text{ if } \frac{a}{b} > 2.4 \quad (C3)$$

where:

- $m = \frac{1}{\nu}$  where  $\nu$  is Poissons ratio
- $a =$  Outer radius of plate
- $b =$  Inner radius
- $t =$  Thickness of plate
- $w =$  Total weight
- $E =$  Young's modulus of elasticity
- $S_r =$  Radial stress
- $S_t =$  Tangential stress

The maximum force transmitted to the plate can be derived as:

$$F_{\text{impact}} = \frac{m V_0 \sqrt{k}}{\sqrt{m+M}} \quad (C4)$$

The gravity effect is neglected, where

- m = Mass of projectile
- M = Mass of target
- k = Stiffness of support plates
- V<sub>0</sub> = Impact velocity of projectile

The values given for the above quantities are:

- m = 0.05/386 16 sec<sup>2</sup>/in
- M = 2/386 16 sec<sup>2</sup>/in
- k = 4682 16/in
- V<sub>0</sub> = 48000 in/sec.

Substituting these values in Equation (C4) gives

$$F_{\text{impact}} = \frac{.05}{386} \times 4800 \sqrt{\frac{4682 \times 386}{(2 \times .05)}}$$
$$= 5837 \text{ lb}$$

Corresponding deflection is given by

$$X = \frac{F_{\text{impact}}}{k}$$

Substituting values gives

$$X = \frac{5837}{4682}$$
$$= 1.25''$$

The maximum stress is  $\sigma_{\text{max}} = 169 \times 5837 = 986453 \text{ psi}$

If thickness is doubled, stiffness increases 9 times and stress by unit load decreases 4 times.

$$F_{\text{impact}} = 3 \times 5938$$
$$= 17511 \text{ lb.}$$
$$\sigma_m = \frac{169}{4} \times 1751$$

C 3

$$= 739839 \text{ psi}$$

Using 4 sandwiched plates

Stiffness is increased 64 times.

Force of impact

$$\begin{aligned} F_{\text{impact}} &= 9 \times 5937 \text{ lb} \\ &= 46696 \text{ lb} \end{aligned}$$

Stress per unit load is decreased 16 times.

$$\begin{aligned} \sigma_{\text{max}} &= \frac{169}{16} \times 46696 \\ &= 493226 \text{ psi} \end{aligned}$$

Using 6 sandwiched plates.

Stiffness is  $6^3$  times stiffness for 1 plate.

$$\begin{aligned} F_{\text{impact}} &= \sqrt{6^3} \times 5837 \text{ lb} \\ &= 14.7 \times 5837 \text{ lb.} \\ &= 85786 \text{ lb.} \end{aligned}$$

Stress per unit load is decreased  $6^2$  times.

$$\begin{aligned} \sigma_{\text{max}} &= \frac{169}{36} \times 85786 \\ &= 402717 \text{ psi} \end{aligned}$$

Sandwiching the plates alone seems impractical so we should try increasing the value of M the weight of the support for target.

As a trial value let M be 30 lb.

Using a sandwich of 6 plates.

$$\begin{aligned} F_{\text{impact}} &= \frac{m V_0 \sqrt{k}}{\sqrt{m+M}} \\ &= 21716 \text{ lb.} \end{aligned}$$

For the sandwich of 6 the corresponding stress per unit load is

$$\frac{169}{36} \text{ psi/lb}$$

$$\sigma_{\max} = \frac{169}{36} \times 21716 = 101944 \text{ psi}$$

$$n = \frac{132}{101.944} = 1.3$$

If the weight of support slab is increased to 62 lb the maximum stress is reduced to

$$\sigma_{\max} = \frac{101944}{1.414} = 72096 \text{ psi}$$

This stress is within the yield strength of AISI 4140 used in plates. The factor of safety  $n$  is given by

$$n = \frac{132}{72.076} = 1.833$$

#### C4. Calibration of the membrane type of force transducer:

Leads from strain gages were connected to terminals of "Switch and Balance" (SB. 10c) unit by which any channel could be selected for testing. The leads from the switch and balance unit were connected to a "Strain Indicator" H.W.D-1 (has built in amplifier) which gives the strain directly. This has outlet for the oscilloscope through a strainert unit.

For loading the membrane to calibrate, a loading frame was designed and fabricated. The frame has two hanging arms at an equidistance from the center of a channel to hold weights.

At the center of the channel a tapered pointer is attached in such a way that it could rest on the aluminum plug. By adding weights to the arms, the membrane could be loaded through the channel and the plug which rests over the knife edge aluminum plug.

To measure the deflection of the membrane, a dial gage of .0005" accuracy and 0.02" range was used. This dial gage was checked for its range and accuracy using a micrometer.

The dial gage tip was arranged in such a way over the membrane to record the axial displacement of the membrane by keeping the dial gage support on a magnetic base. The magnetic base was attached to the supporting pipe to avoid the relative displacement of the pipe support due to the load.

Each channel of the strain gage circuit was balanced properly. The signal from the strain indicator was connected to the oscilloscope (Tektronix 535A) with Dual plug in unit 1.A.1.

The membrane was calibrated for load and deflection using the readings of the scope, load and the dial gage readings for the deflection of the membrane. The best set of readings from the strain gage (Radial one of Rosette  $R_2$ ) with terminals No. 25 and 26 was taken for calibration. Also the strain gage (Radial one of rosette  $R_1$ ) with terminals No. 15 and 16 was used to calibrate the membrane.

On comparing the responses for the load, it was found the gage with terminals No. 25 and 26 gave realistic response than any other gage. The readings were tabulated as shown in table C1 and C2. The graph of calibration was drawn with these readings as shown in Figure C7 and C8.

#### Beam Transducer:

This is basically a steel beam of 2" x 1/2" cross section and a span of 24" fixed by bolts over two cast steel legs forming a fixed-fixed beam of 24" span. As shown in figure 11. This type of transducer was designed to overcome some flaws that the membrane had. To say a few advantages, 1. This transducer has easy accessibility on all sides. 2. Mounting the specimen over the transducer was made easy by this arrangement, 3. With single beam. the measurement of deflection of the beam to load with dial gage for calibrations made easy. 4. Mounting strain gages on both top and bottom surfaces was made easy.

Four (4) strain gages of each 1000 resistance on paper back were mounted to the beam using Eastman 910 contact cement. Two gages on the top surface and two at the bottom surface. Each gage is at a distance of 4" from the center of the beam. That is two gages on compression and two gages in tension.

To avoid any mishap to the strain gages while testing, they were covered with insulation tapes and then wrapped around with special tapes.

For mounting the specimen over the transducer, a fixture was designed and fabricated. This has got a vise which can grip over the specimen in such a way that the specimen is at the midspan of the beam.

#### C5. Calibration of the beam type of transducer:

For the calibration of the beam transducer, the Baldwin-machine (universal testing machine) was used for loading the beam. Oscilloscope type 549 with a special Q plug in unit was used. This special Q plug built in Wheatstone bridge, oscillator, to give excitation and built in amplifiers. Also a dial gage of 0.001" accuracy with 0.250" range was used.

The beam was loaded using the Baldwin machine in the low range setting. The dial gage tip was centered exactly to the center of the beam to measure the deflection of the beam for any given load. The strain gages were connected to the oscilloscope and balanced following the steps in sequence to balance the bridge of the scope for

null deflection. The scope was set at 10 per division and the static calibration was started by loading the beam at different loads noting the scope trace deviation and the dial gage readings. The readings were tabulated as given in Table C3.

With the readings taken for calibration, the necessary graphs of calibration were drawn as shown in figure 09. On studying the readings, it was found that beyond 400 lbs load, the readings of scope started creeping. The reason being the support legs of the single beam transducer started sliding and widening the gap of the support on the Baldwin machine.

It was then decided to increase the rigidity of the support of the beam dual beam transducer was selected for testing. The arrangement is the same as that of the single beam except for the additional beam interconnecting the legs of the single beam transducer. The same calibration curve holds good for this also since the new arrangement doesn't change the boundary conditions of the previous one.

Table C1. Readings for Calibration of membrane with Strain Gage having terminals #25 and 26.

Load lbs.	On Loading	Scope Divisions from reference in cm				dial reading
		Unloading	Loading	Unloading	Loading	
4.4	0	0.1	0	0.3	0.3	15.5
8.8	0.3	0.3	0.5	0.6	0.6	11.5
13.2	0.5	0.5	0.8	0.9	0.9	11.5
17.6	0.6	0.5	1.0	1.0	1.0	9.5
22	0.6	0.6	1.1	1.1	1.1	8.75
26	0.7	0.6	1.1	1.1	1.1	7.25
32	0.7	0.7	1.2	1.2	1.2	5.0
38	0.7	0.7	1.3	1.3	1.3	4.25
40	0.7	0.7	1.4	1.4	1.4	2.5

Table C2

The data taken for making graph of calibration of the membrane transducer for load & deflection

Load lbs	Scope Deflection cm	Dial Gage Reading mils
4.4	0.3	0
8.8	0.6	4x0.5
13.2	0.9	4x0.5
17.6	1.0	6x0.5
22	1.1	6.75x0.5
26	1.1	8.25x0.5
32	1.2	10.5x0.5
38	1.3	11.25x0.5
40	1.4	



Table C3. Readings for the Calibration of Beam Transducer for Load and Deflection.

Load lbs.	Scope Division	Dial Gage Reading	Beam Transducer deflection in mils
0	0	9	0
100	0.7	22	13
200	1.9	51	42
300	2.2	74	65
400	2.8	104	95
500	2.6	137	128
600	2.8	173	164

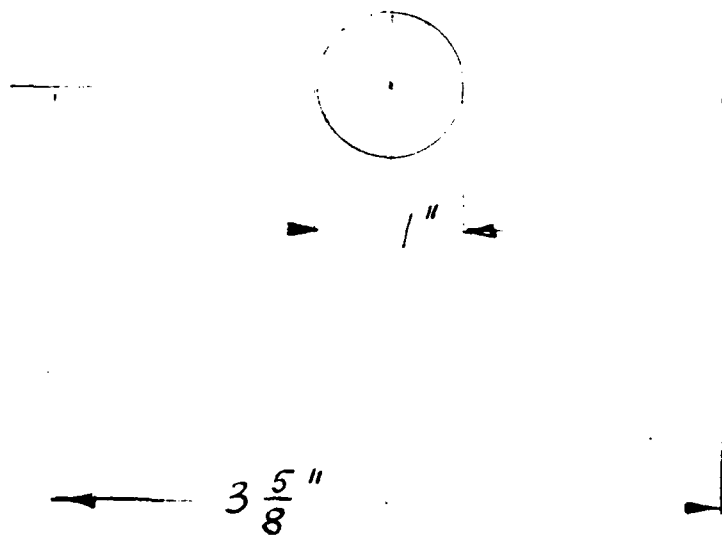


Fig. C1. Membrane of the transducer.

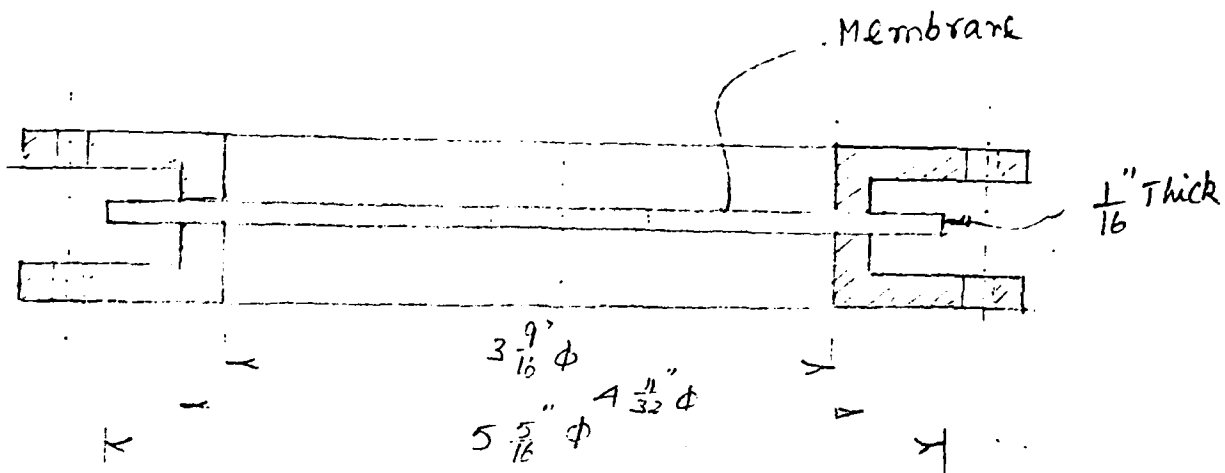


Fig. C2. Membrane clamped between two flanges.

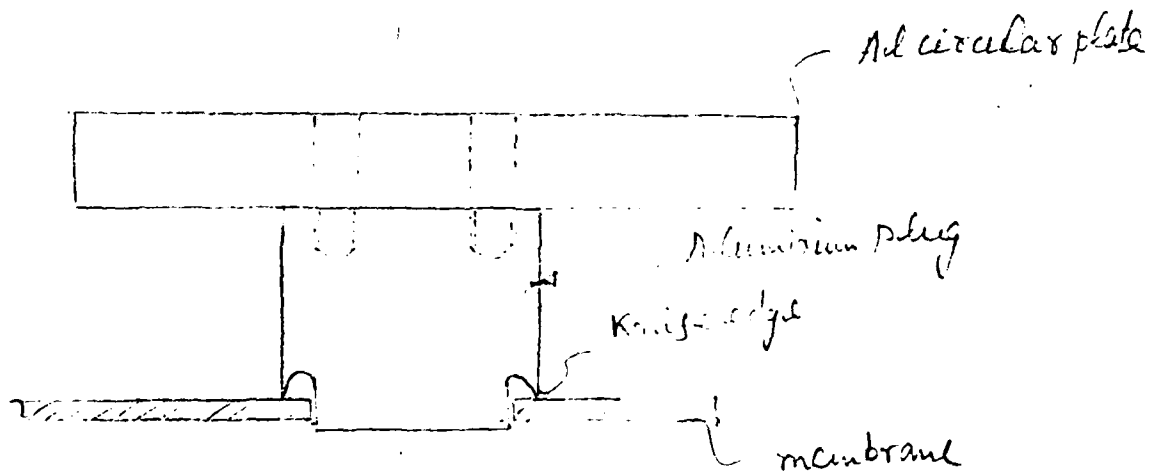


Fig. C3. Al. Plug with knife edge that fits over membrane.

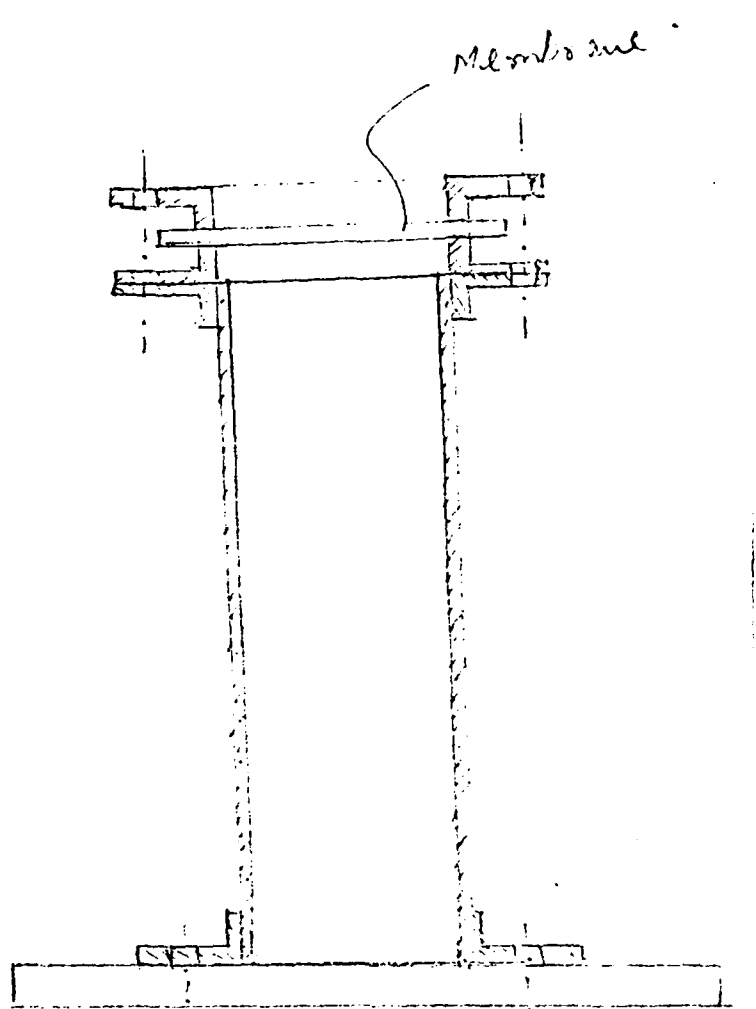


Fig. C4. Membrane with flanges attached to support pipe and Al. base.

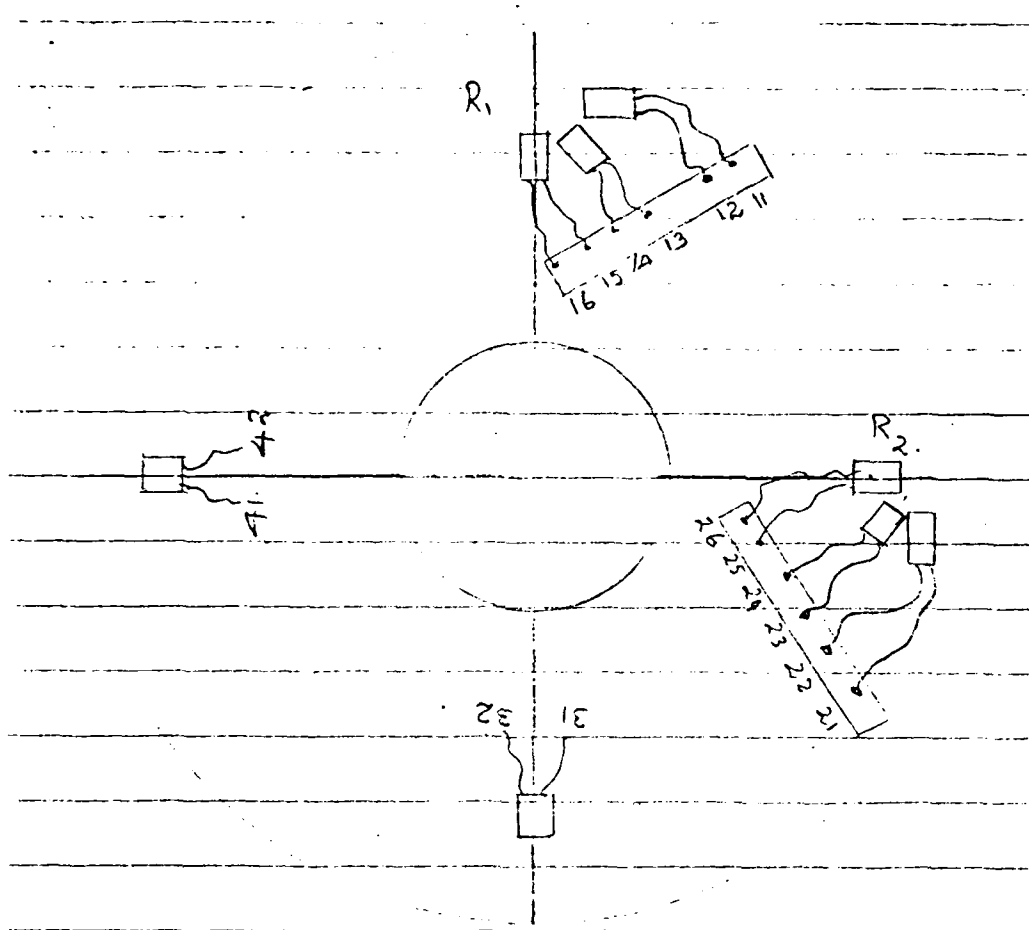


Fig. C5. Strain gages on the membrane.

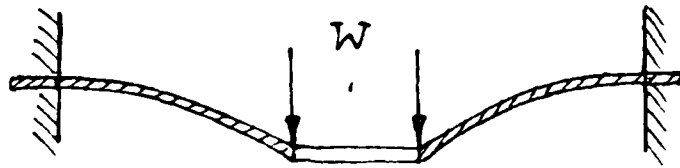


Fig. C6. Schematic diagram of the membrane force transducer.

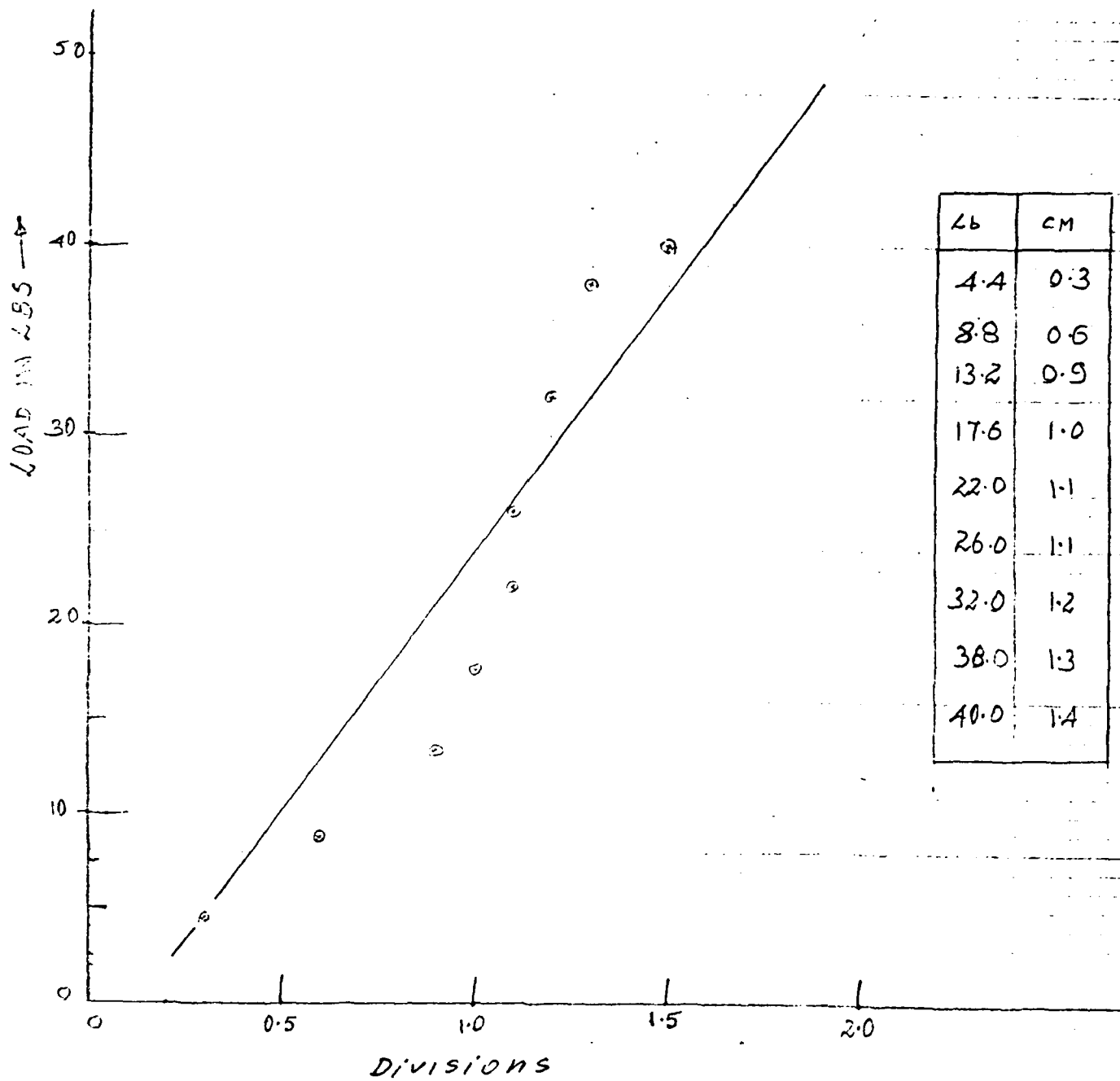
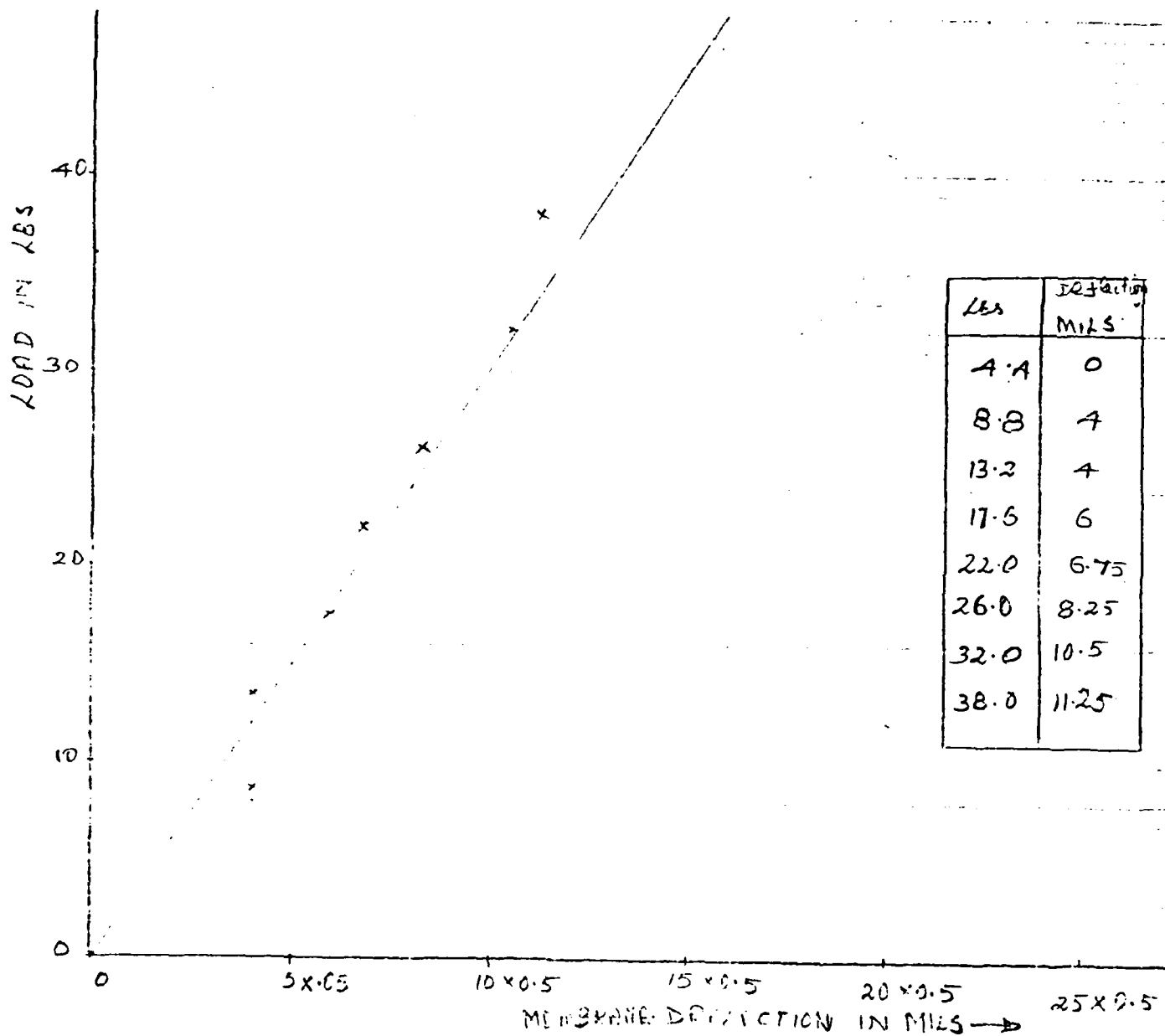


Fig. C7. Membrane Calibration curve for strain gage with terminals # 25 & 26 Channel 3. Scope with 0.1V/cm.



.Fig. C8. Membrane 1. case transducer calibration curve for load vs. membrane deflection.



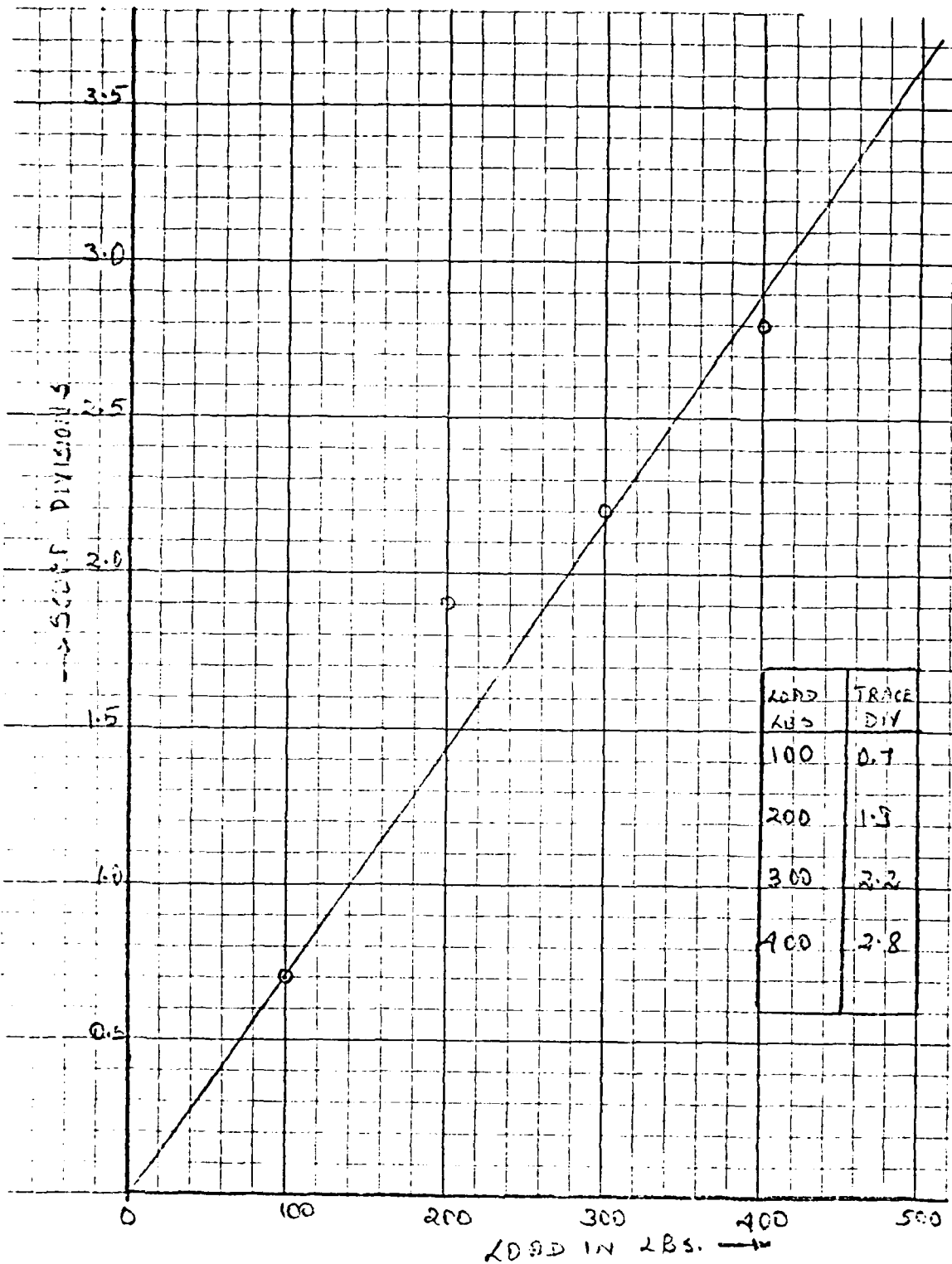


Fig. C9. Force transducer calibration curve.

## APPENDIX D

### THE DEPTH OF PENETRATION IN A TARGET AND MAXIMUM FORCE IN SUPPORT PLATE FOR A LEAD-LEAD IMPACT EXPERIMENT

Experimental data from Summers and Charters (Ref. 2) are used to find the depth of penetration for various combinations of target material and penetrator material. Arguments are then advanced to show that the force time curve in impact can be idealized to a right triangular shape. The duration of impact is also estimated and they response in the supporting spring is found by convolution.

#### D1. DEPTH OF PENETRATION

The empirical relationship for depth of penetration is given by Summers and Charters as

$$\frac{P}{d} = 2.28 \left( \frac{\rho_P V}{\rho_T a_T} \right)^{\frac{2}{3}} \quad (D1)$$

$P$  = depth of penetration.

$d$  = Diameter of penetrator

$v$  = Velocity of penetrator

$a_t$  = Bar velocity of sound in target.

$\rho_P/\rho_T$  = Density ratio of penetrator to target.

Here the effect of the latent heat of the materials are lumped into the term  $\sqrt{a_T}$ .

Using typical quantities for a lead-lead impact

$$\frac{P}{1 \text{ cm}} = 2.28 \left( \frac{5000}{4100} \right)^{\frac{2}{3}}$$

$P = 2.6 \text{ cm.}$

D1

## D2. Elementary Phenomenology of Quasi-One Dimensional Impact.

Assuming penetrator has a plane front the compressive shock wave is reflected from the edges as a rarefaction shock wave and travels toward the center of the front of penetrator causing stress relief. The quasi-one dimensional impact stops when this when this rarefaction wave reaches the center.

Referring to the Hugoniot for lead the speed of this wave is for an initial speed of projectile of 5000 ft/sec. is given by

$$V = \frac{5000}{2} = 2500 \text{ ft/sec.}$$

Time to reach center :

$$\begin{aligned} \frac{t}{\tau} &= \frac{\text{distance}}{\text{speed}} = \frac{.5 \text{ cm} \times \frac{1 \text{ in}}{2.54 \text{ cm}}}{2500 \text{ ft/sec} \times \frac{12 \text{ in}}{1 \text{ ft}}} \\ &= 6.6 \text{ } \mu\text{s} \end{aligned}$$

This ends the primary phase.

## D3. Bernoulli Flow

Simultaneous with quasi-one dimensional flow is Bernouilli flow in the stress relieved portions of penetrator and target this flow continues after quasi-one dimensional impact till penetration stops.

The stagnation pressure due to this flow is derived from the equation

$$P_s = 1/2 \rho U^2 \quad (D2)$$

$P_s$  = stagnation pressure

$\rho$  = density of material at the high pressure

$U$  = Interface velocity.

The stagnation pressure due to Bernouilli flow is much less than the contact pressure on the Hugoniot.

D4. Forces due to contact pressure and stagnation pressure

If the pressure as read from the Hugoniot is  $P_H$  then the force on target due to this pressure is

$$F_H = P_H A. \quad \text{where } A \text{ is area undergoing quasi one dimensional impact.}$$

Now, for a cylindrical penetrator

$$A = \frac{\pi}{4} d^2$$

The area undergoing quasi-one dimensional impact is the total area minus the stress relieved portions.

$$\text{i.e.} \quad A = \pi \left( \frac{d}{2} - vt \right)^2 \quad (D3)$$

where  $V$  is the velocity of the rarefaction wave and  $t$  is the time.

$$F_H = \pi P_H \left( \frac{d}{2} - vt \right)^2 \quad (D4)$$

The area with the stagnation pressure  $P_s$  is given by

$$A_s = \pi \left( \frac{d}{2} \right)^2 - \pi \left( \frac{d}{2} - vt \right)^2 = \pi vt(d - vt)$$

Total force

$$\begin{aligned}
 F_T &= F_H + F_S \\
 &= \pi P_H \left( \frac{d}{2} - vt \right)^2 + \pi P_S \left( \frac{d}{2} \right)^2 - \pi P_S \left( \frac{d}{2} - vt \right)^2 \\
 &= \pi (P_H - P_S) \left( \frac{d}{2} - vt \right)^2 + \pi P_S \left( \frac{d}{2} \right)^2
 \end{aligned}$$

where:

$P_H$  is constant and drops to zero when  $Vt = \frac{d}{2}$

$P_S$  is a decreasing function of time,

at  $t = 0$

at same time  $t_1$  when  $P_S$  has decreased to zero and  $P_H$  is already zero.

$$F_T = 0$$

The impact force can thus be idealized by the graph shown in Figure D1.

#### D5. Formulae for depth of penetration

Various empirical formulae for penetration exists. The most well known being the formula given by Summers and Chartres. Ref 2

Penetration ratio in this formula is given by (Eq. D1)

$$\frac{P}{d} = 2.28 \left[ \left( \frac{\rho_P}{\rho_T} \right) \left( \frac{V}{a_T} \right) \right]^{2/3} \quad (D1)$$

$P$  = penetration depth

$d$  = Characteristic diameter

$\rho$  = Densities for projectile and target.

$V$  = Velocity of projectile

$a_T$  = Speed of sound in target.

For a lead-lead impact  $\frac{\rho_P}{\rho_T} = 1$

and  $\frac{P}{d} = \frac{2.28}{a_T^{2/3}} V^{2/3}$

and  $P = \frac{2.28}{a_T^{2/3}} \cdot d \cdot V^{2/3}$

Characteristic diameter is given by

$$d = 2 \left( \frac{3V}{4\pi} \right)^{\frac{1}{3}}$$

where:  $V$  is volume of penetrator

Typically the dimensions of the bullet used in impact can be approximated by a small solid cylinder of the dimensions .25" Dia and .44" long.

The shape of the leading edge of bullet is not a determining factor in penetration depth for high velocity penetration. With the given dimensions.

$$d = 2 \times \left( \frac{3 \times \pi \times .25^2/4 \times .44}{4\pi} \right)^{\frac{1}{3}}$$

$$d = 2 \times (.1727) = .3455 \text{ "}$$

$$\begin{aligned} \therefore P &= \frac{2.28}{a_T^{2/3}} \times .3455 \times V^{2/3} \\ &= .0031 V^{2/3} \end{aligned}$$

Taking  $V$  as 5000 ft/sec.

$P = .9$ ". This figure can be compared with actual penetration figures.

Alternatively the depth of penetration can be found by assuming that the volume of crater formed is hemispherical and proportional to the kinetic energy of the projectile. Using this depth of penetration ( $d$ ) is given by

$$d = \left( \frac{6V}{\pi} \right)^{\frac{1}{3}}$$

but

$$V = k_1 \frac{1}{2} m V^2$$

25

$k_1$  is the volume of material removed/unit kinetic energy.

$$d = \left( \frac{3 k_1}{\pi} \right)^{1/3} m^{1/3} V^{2/3}$$

For lead  $k_1 = \frac{3.31}{10^4} \text{ in}^3/\text{ft-lb}$

Also  $m = \frac{\pi \times .25^2 \times .44}{4} \times \frac{705}{32.2 \times 144 \times 12}$

$$= .0002735 \text{ lb}^2/\text{ft}$$

$$d = .068 \times .065 \times V^{2/3}$$
$$= .00442 V^{2/3}$$

Using  $V = 5000 \text{ ft/sec}$ .  $d = 1.29''$ .

A third method for finding depth of penetration is to find crater volume as previously and that the volume assumed by crater is as drawn.

Volume therefore is

$$V = k_1 \cdot \frac{1}{2} m V^2 = 3.31 \times 10^{-4} \times .5 \times .0002735 \times 6000^2$$
$$= 1.1316 \text{ m}^3$$

$$R = .64''$$

$$d = .64 + .44 = 1.08''$$

All these methods give different answers but the empirical results are of course more trustworthy.

D6. Correlation of crater volume with penetrator energy and latent

heat of fusion of material.

For the case selected for lead-lead impact. The kinetic energy of the penetrator has been calculated as 6415 ft - lb.

Also

$$V = 2.12 \text{ in}^3$$

The energy required for complete melting of such a volume is

$$E = \rho V L$$

where L is the latent heat of fusion.

For lead  $L = 10 \text{ BTU/lb.}$

Since  $E_{\text{kinetic}} = 6415 \text{ ft-lb.}$

and  $778 \text{ ft-lb} = 1 \text{ BTU}$

$6415 \text{ ft-lb} = 6415/778 \text{ BTU}$

$= 8.245 \text{ BTU}$

If all this energy goes into melting a mass corresponding to the crater volume.

Then

$$8.245 = \frac{V \times 705}{144 \times 12} \times 10$$

$$= 4.01 \times V$$

$$\therefore V = \frac{8.245}{4.01} = 2.02 \text{ in}^3$$

The actual crater volume calculated from empirical formula as 1.13 in<sup>3</sup>. This shows a lot of energy is lost by shock and other modes of energy involved.

Recalculation of mass of lead bullet

Mass = Volume  $\times$  density

$$= \frac{\pi \times .25^2 \times .44}{4} \times \frac{705}{144 \times 12} \cdot \frac{1}{32} = 0.0002754 \text{ lb}^2/\text{ft}$$

D7



D7. Momentum and impulse

The momentum of the bullet is given by

$$\begin{aligned} mV_0 &= .0002754 \times 5000 \\ &= 1.377 \text{ lb-s} \end{aligned}$$

Equating this to

$$t_1 = 2 \times \frac{1.377}{F_0}$$

A speed of 5000 ft/sec. = 1.524 km/sec.

For this speed range the shock Hugoniot is almost a straight line for lead.

For 1.524 km/s the reflected Hugoniot intersects the Hugoniot at about .35 megabars.

.35 megabars.

$$\begin{aligned} &= .35 \times 14.7 \times 10^6 \text{ psi.} \\ &= 5145000 \text{ psi.} \end{aligned}$$

The area of projectile is

$$\frac{\pi \times .25^2}{4} = 0.049 \text{ in}^2$$

$$\begin{aligned} F_0 &= 5145 \times .049 \text{ lb.} \\ &= 252000 \text{ lb.} \end{aligned}$$

$$t_1 = \frac{2 \times 1.377}{252000}$$

$$t_1 = 1.1 \times 10^{-5}$$

D8 Response of spring support

The actual response of the support spring can be found by convolution where

$$x(t) = \int_0^{t_1} \frac{F(\xi)}{m\omega_n} \sin \omega(t - \xi) d\xi$$

$$\text{Here } F = F_0 \left( 1 - \frac{t}{t_1} \right)$$

m is mass of target and  $\omega_n$  the natural frequency of vibration of the spring mass system

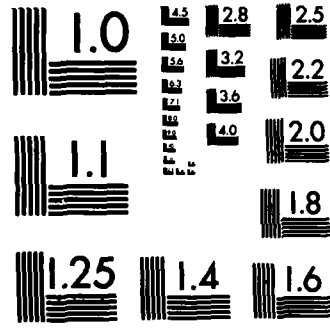
DP

The max force in the spring is found by finding  $x_{\max}$

and then  $F_{\max} = k \cdot x_{\max}$

AD-A123 562 VISCOELASTIC AND DAMPING PROPERTIES OF ARMOR MATERIALS 2/2  
UNDER HYPERVELOCITY PENETRATION(U) TUSKEGEE INST AL  
SCHOOL OF ENGINEERING C A BRONIAREK 31 DEC 82  
UNCLASSIFIED ARO-18447.1-EG-N DAAG29-81-G-0007 F/G 19/4 NL

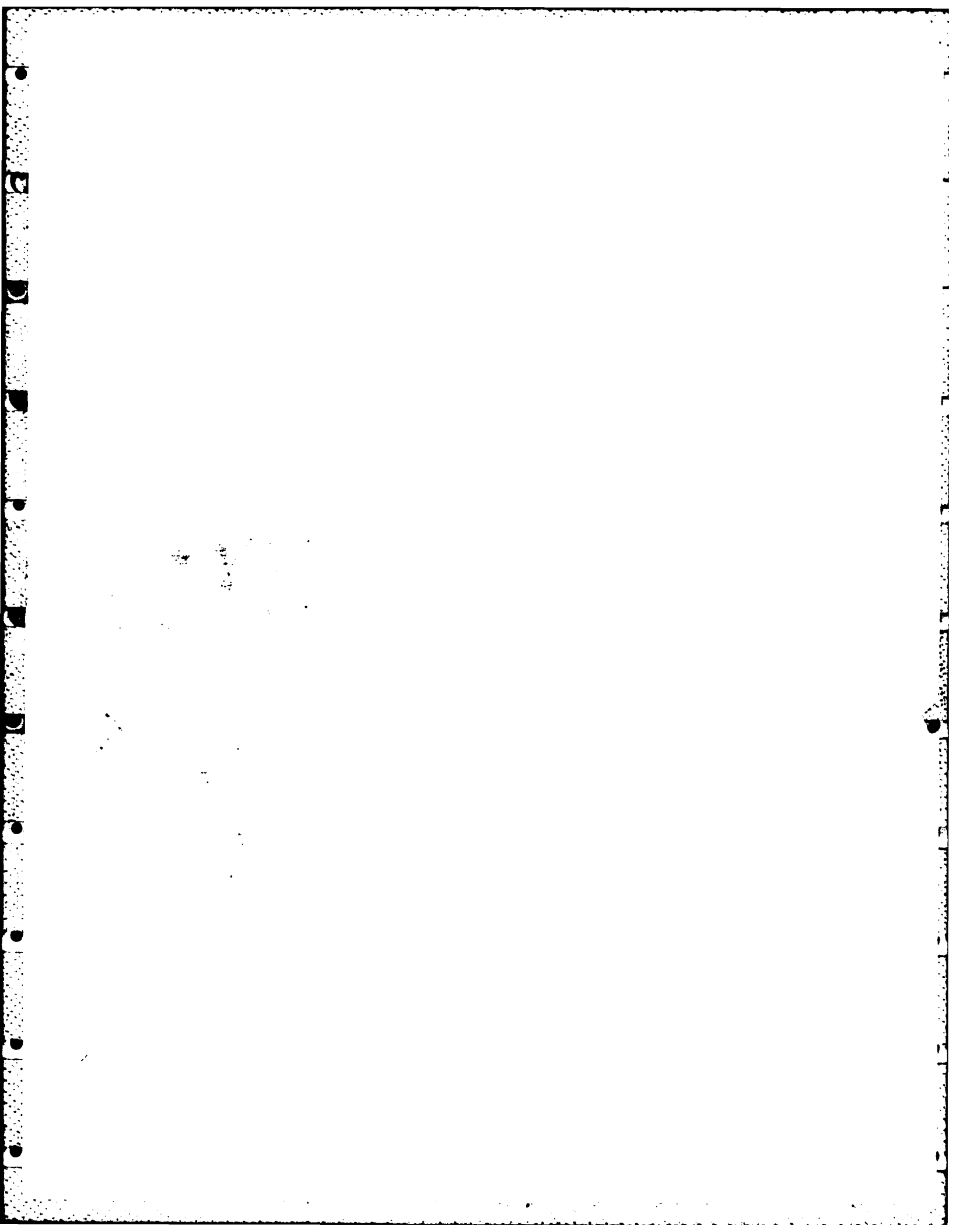
END  
FILMED  
DTIC



MICROCOPY RESOLUTION TEST CHART  
NATIONAL BUREAU OF STANDARDS-1963-A

## REFERENCES

1. Zukas, J.A. Impact Dynamics, reprint from "Emerging Technologies in Aerospace Structures, Design, Structural Dynamics and Materials" ASME, publication, Edited by, J.R. Vinson, pp - 161 - 198.
2. Baker, W.E. Westine, P.S., and Dodge, F.T., Similarity Methods in Engineering Dynamics, Hayden Book Company, Inc., Rochelle Park, New Jersey
3. Goldsmith, W. Impact, Edward Arnold, London, 1960
4. Summers, J.L and Charters A.C., "High-speed Impact of Metal Projectiles in targets of various materials," Proceedings of Third Symposium on Hypervelocity Impact, 1, pp 101-110, Feb. 1959.
5. Roark, R. J. Formulas for Stress and Strain, McGraw-Hill Co. 1938.
6. Constitutive Equations in Viscoplasticity: Phenomenological and Physical Aspects, ASME publication AMD-Vol. 21, 1976.



2-8

DT